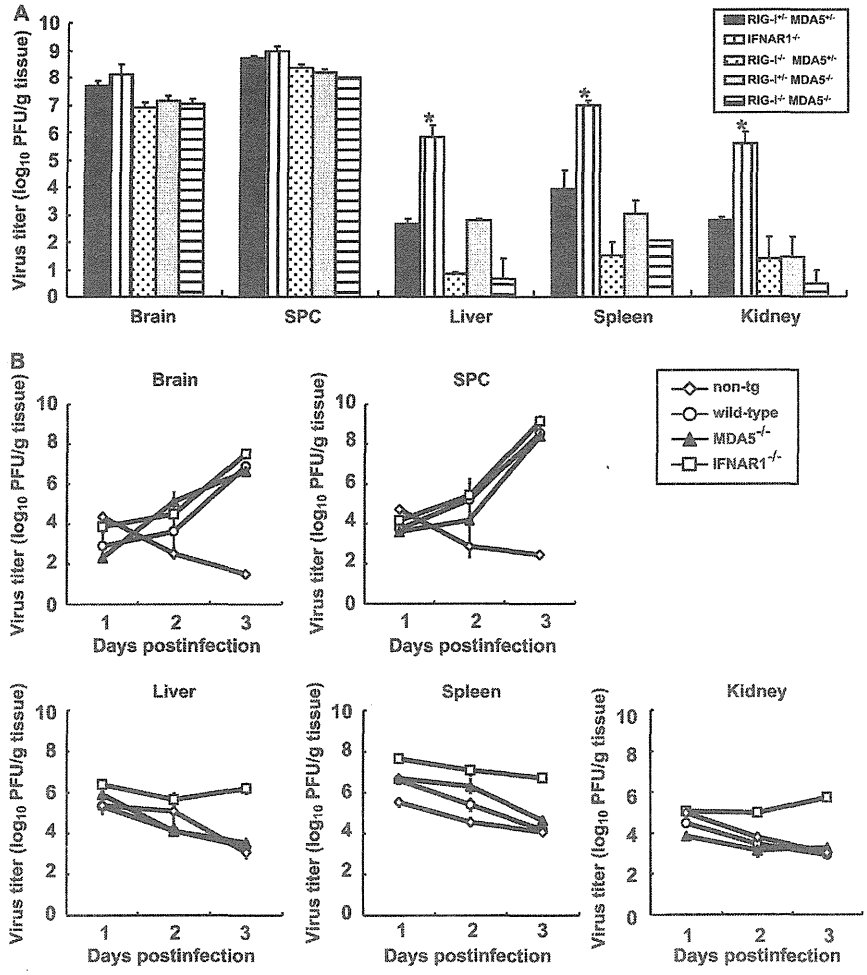

FIG 4 (A) PV replication in RIG-I- and MDA5-deficient mice. RIGI-I$^{+/-}$ MDA5$^{+/-}$, RIGI-I$^{-/-}$ MDA5$^{+/-}$, RIGI-I$^{-/-}$ MDA5$^{+/-}$, and RIGI-I$^{-/-}$ MDA5$^{-/-}$ mice in the ICR background and IFNAR1$^{-/-}$ mice in the B6 background ($n = 3$) were intravenously infected with 2×10^7 PFU of PV. Infected mice were paralyzed or dead at 3 to 5 days postinfection. The tissues of the paralyzed mice were collected, and the viral titers were determined using a plaque assay (*, $P < 0.01$ by t test compared to RIGI-I$^{+/-}$ MDA5$^{+/-}$ mice). (B) PV replication kinetics in MDA5-deficient mice. Nontransgenic (non-tg) mice, wild-type mice, MDA5$^{-/-}$ mice, and IFNAR1$^{-/-}$ mice in the B6 background ($n = 3$) were infected as described above. Tissues were collected daily, and viral titers were determined. SPC, spinal cord.

PV replication in nonneural tissues and mortality rates of mice deficient in RIG-I-like receptors. We have previously shown that the IFN-α/β response forms an innate immune barrier to prevent PV replication in nonneural tissues and PV invasion of the CNS (19, 25). Therefore, we evaluated PV replication in neural and nonneural tissues in RLR-deficient mice. The mice were infected with 2×10^7 PFU of PV, which is approximately 100 times higher than the 50% lethal doses for all mouse strains. The infected mice showed paralysis by 3 to 5 days postinfection. The brain, spinal cord, liver, spleen, and kidney of the paralyzed mice were recovered, and their viral titers were determined (Fig. 4A). PV was recovered from the CNS of the paralyzed mice almost equally among the genotypes. The viral titers recovered from the liver, spleen, and kidney of IFNAR1$^{-/-}$ mice were significantly higher than those of wild-type mice, as previously described (19). However, PV titers that were recovered from these organs of RIG-I$^{-/-}$ MDA5$^{+/-}$, RIG-I$^{+/-}$ MDA5$^{-/-}$, and RIG-I$^{-/-}$ MDA5$^{-/-}$ mice were as low as or lower than those in the organs of RIG-I$^{+/-}$ MDA5$^{+/-}$ mice. We then examined virus replication kinetics using nontransgenic mice, wild-type mice, IFNAR$^{-/-}$ mice, and MDA5$^{-/-}$ mice in the B6 background (Fig. 4B). The viral load in the CNS increased in a similar fashion among the transgenic mouse strains. However, the viral load kinetics in the liver, spleen, and kidney of wild-type and MDA5$^{-/-}$ mice were similar to those of nontransgenic mice. The values for nontransgenic mice indicate the kinetics of clearance of inoculated virus. The results indicated that PV replication was severely inhibited in the liver, spleen, and kidney of wild-type and MDA5$^{-/-}$ mice. This inhibition correlated well with the induction of serum IFNs in MDA5$^{-/-}$ mice (Fig. 2). The PV antigen was detected in neurons in the CNS but not in other tissues in all knockout mice (Table 1). This result indicates that the lack of RLRs did not alter the tissue tropism of PV. These data suggest that inhibition of PV replication in nonneural tissues is not dependent on RLRs and that MDA5-independent mechanisms are the major contributors in controlling PV replication.

We examined the mortality rates of RIG-I$^{+/-}$ MDA5$^{+/-}$, RIG-I$^{-/-}$ MDA5$^{+/-}$, RIG-I$^{+/-}$ MDA5$^{-/-}$, and RIG-I$^{-/-}$ MDA5$^{-/-}$

TABLE 1 PV antigens in RIG-I- and MDA5-deficient mice

Organ or tissue	No. of PV antigen-positive mice/no. of mice tested			
	RIG-I$^{+/-}$ MDA5$^{+/-}$	RIG-I$^{-/-}$ MDA5$^{+/-}$	RIG-I$^{+/-}$ MDA5$^{-/-}$	RIG-I$^{-/-}$ MDA5$^{-/-}$
Brain	4/4	3/3	4/4	4/4
Spinal cord	4/4	3/3	4/4	4/4
Heart	0/4	0/3	0/4	0/4
Lung	0/4	0/3	0/4	0/4
Liver	0/4	0/3	0/4	0/4
Kidney	0/4	0/3	0/4	0/4
Spleen	0/4	0/3	0/4	0/4
Pancreas	0/4	0/3	0/4	0/4
Intestine	0/4	0/3	0/4	0/4
Adipose tissue	0/4	0/3	0/4	0/4

mice in the ICR background after intravenous infection with PV at 10^3, 10^4, and 10^5 PFU (Fig. 5A, B, and C). The mortality rates of these mice did not differ significantly from each other. We observed that the mortality rates of RIG-I$^{+/-}$ MDA5$^{-/-}$ mice that were inoculated with 10^4 PFU of PV was slightly higher than the mice of other genotypes. However, significant differences were not observed in mice that were inoculated with the other doses. Similar experiments were performed using MDA5$^{-/-}$ and MDA5$^{+/-}$ mice in the B6 background (Fig. 5D, E, and F). We did not observe significant differences between the MDA5$^{-/-}$ and MDA5$^{+/-}$ mice. The mortality rate of MDA5$^{-/-}$ mice was slightly higher than that of MDA5$^{+/-}$ mice that were inoculated with 10^5 PFU of PV. However, the opposite trend was observed when mice

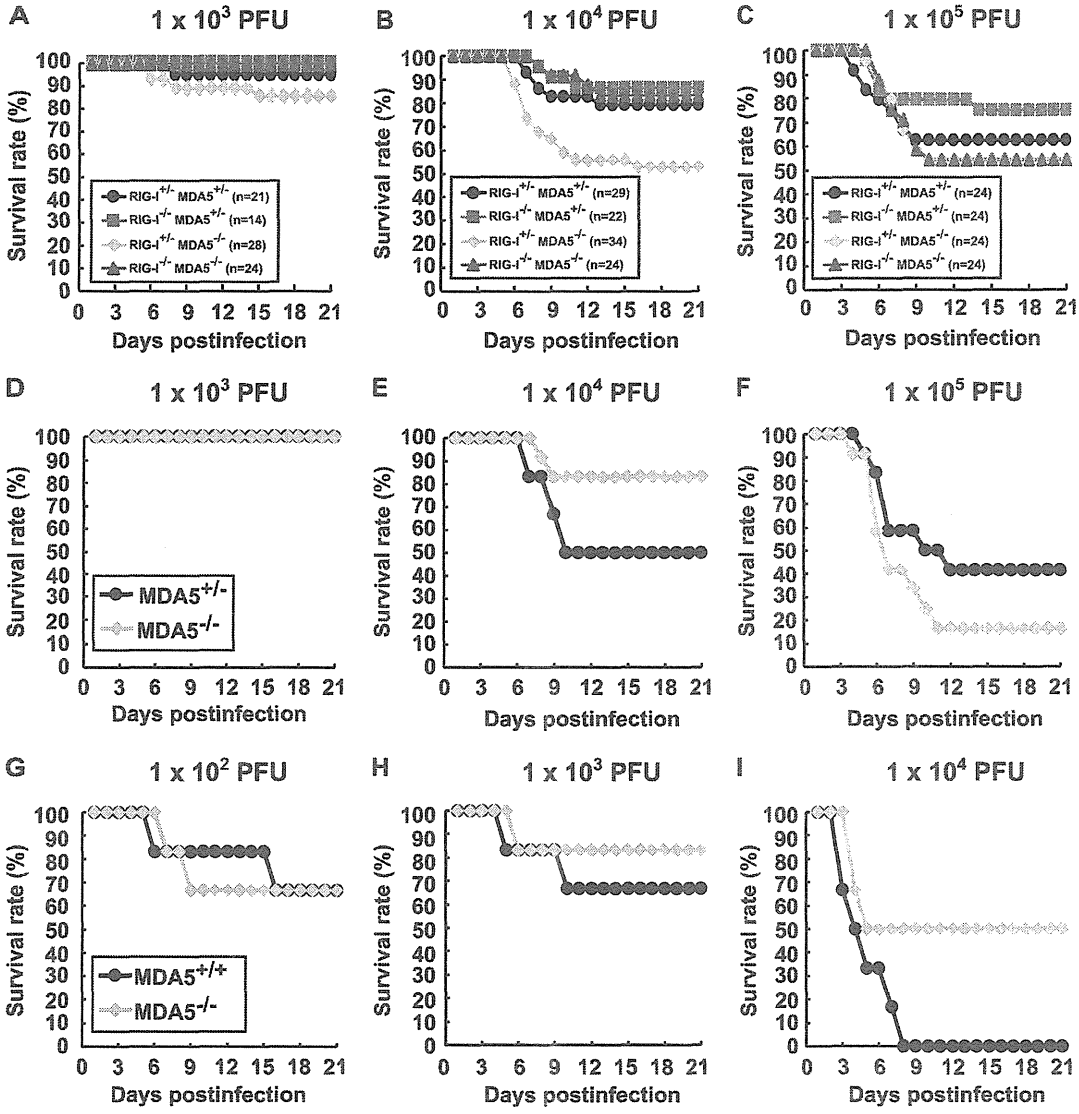

FIG 5 Mortality rates of RIG-I- and MDA5-deficient mice. Littermates of the genotypes indicated were obtained by mating RIGI-I$^{+/-}$ MDA5$^{+/-}$ and RIGI-I$^{-/-}$ MDA5$^{-/-}$ mice in the ICR background. The mice were infected intravenously with 10^3 (A), 10^4 (B), or 10^5 (C) PFU of PV. The results shown are the sums of several independent experiments. The total numbers of mice of the different genotypes that were used are boxed, and the doses used are shown at the top. Littermates of MDA5$^{+/-}$ and MDA5$^{-/-}$ mice were obtained in the B6 background. The mice (n = 12) were intravenously infected with 10^3 (D), 10^4 (E), or 10^5 (F) of PV. MDA5$^{+/+}$ and MDA5$^{-/-}$ mice (n = 6) were intracerebrally infected with 10^2 (G), 10^3 (H), or 10^4 (I) PFU of PV, respectively. We monitored the survival rates of the mice for 3 weeks after infection.

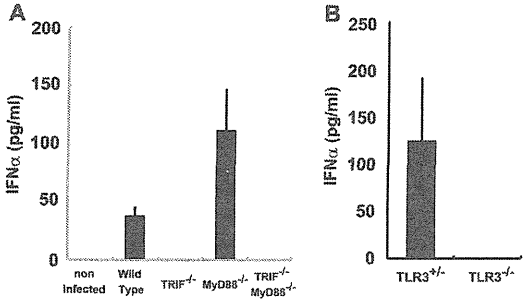

FIG 6 Production of serum IFN-α in TRIF-, MyD88-, and TLR3-deficient mice. Mice (n = 3 or 8) were intravenously infected with 10^7 PFU of PV. IFN-α levels of TRIF- and MyD88-deficient mice (A) and TLR3-deficient mice (B) at 12 hpi were compared. The experiments were repeated twice, and representative data are shown.

were inoculated with 10^4 PFU of PV. We suspect that the slight difference between the mortality rates of wild-type and MDA5$^{-/-}$ mice was in the range of experimental fluctuation, and thus, the disruption of MDA5 did not significantly influence the mortality rate. In order to determine if the same is true when mice are infected by other routes, we inoculated wild-type and MDA5$^{-/-}$ mice with PV intracerebrally and compared their mortality rates (Fig. 5G to I). Their mortality rates did not differ significantly. These results suggest that MDA5 does not make a great contribution to the protection of mice, at least after intracerebral and intravenous infections. Taken together, the MDA5-mediated response does not play a dominant role in IFN production, ISG induction, or inhibition of PV replication *in vivo*, unlike the MDA5-mediated effects on EMCV infection.

IFN response in TRIF- and MyD88-deficient mice. Because the experiments with MDA5-deficient mice suggested the existence of other protective mechanisms in PV infection, we investigated the role of TLRs using TRIF- and MyD88-deficient mice. PVR-tg mice were mated with TRIF$^{-/-}$ and/or MyD88$^{-/-}$ mice in the B6 background. Serum IFN-α of mice infected with 10^7 PFU of PV was measured using ELISA at 12 hpi (Fig. 6A). Interestingly, serum IFN production in response to PV infection was abrogated in TRIF$^{-/-}$ mice. Because TRIF acts as an adaptor for TLR3 and TLR4, we tested whether the same phenomenon occurs in TLR3$^{-/-}$ mice. Serum IFN induction was not observed in TLR3-deficient mice (Fig. 6B). These results suggest that the TLR3-mediated pathway is essential for IFN production in response to PV infection.

We next assessed the induction of mRNAs for OAS1a (Fig. 7A) and IRF-7 (Fig. 7B) in various organs using real-time RT-PCR. The induction of OAS1a and IRF-7 was observed in all mice. Although serum IFN production was abrogated in TRIF$^{-/-}$ mice and TRIF$^{-/-}$ MyD88$^{-/-}$ mice (Fig. 6), a significant level of ISG mRNA was induced. However, the induction levels were slightly lower than those in wild-type mice in some cases. The results suggest that the TRIF-mediated pathway contributes to ISG expression mainly through the induction of serum IFNs in response to PV infection and that some other mechanisms may also contribute to ISG expression.

PV replication in nonneural tissues and mortality rates of TRIF- and MyD88-deficient mice. The brain, spinal cord, liver, spleen, and kidney of paralyzed mice were recovered, and viral titers were determined (Fig. 8). PV was recovered from the CNS of TRIF$^{-/-}$, MyD88$^{-/-}$, and TLR3$^{-/-}$ mice, and the titers were not different from those of wild-type mice. However, the viral titers of the liver, spleen, and kidney of TRIF$^{-/-}$ and TLR3$^{-/-}$ mice were significantly higher than those of wild-type mice but lower than those of IFNAR1$^{-/-}$ mice. We then examined the virus replication kinetics in TRIF$^{-/-}$ mice (Fig. 8B). The viral load in the CNS increased in TRIF$^{-/-}$ mice similarly to that in other mice. In accordance to the absence of serum IFN (Fig. 2), the viral loads in the liver, spleen, and kidney of TRIF$^{-/-}$ mice increased, while the viral loads in these organs of wild-type mice decreased. PV antigens were detected in the CNS of all of the knockout mice. In addition, PV antigens were detected in the adipose tissue, pancreas, and kidney of several TRIF$^{-/-}$ and MyD88$^{-/-}$ mice (Table 2). These results suggest that these tissues support viral multiplication in these knockout mice and that the TLR-mediated signaling pathways contribute to the regulation of PV replication in nonneural tissues.

The mortality rates of TRIF$^{-/-}$, MyD88$^{-/-}$, and TLR3$^{-/-}$

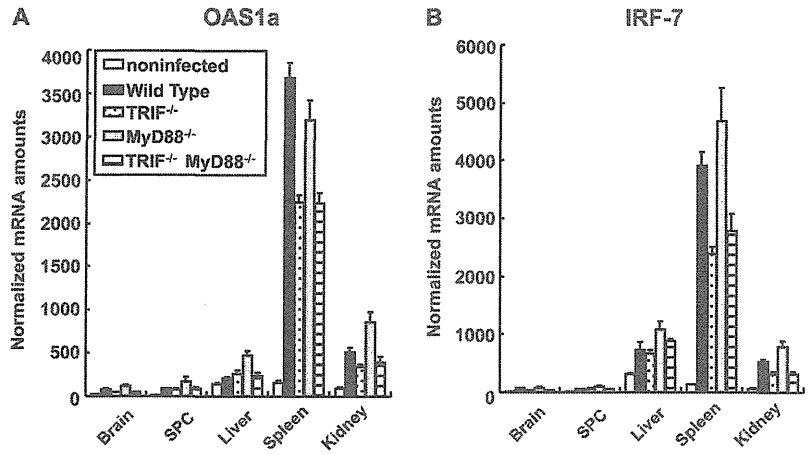

FIG 7 ISG induction in TRIF- and MyD88-deficient mice. Mice (n = 4) were intravenously infected with 10^7 PFU of PV. At 12 hpi, RNA was isolated from the indicated tissues of the infected mice and OAS1a (A) and IRF-7 (B) mRNA levels were determined by quantitative real-time PCR. The experiments were repeated twice, and representative data are shown. SPC, spinal cord.

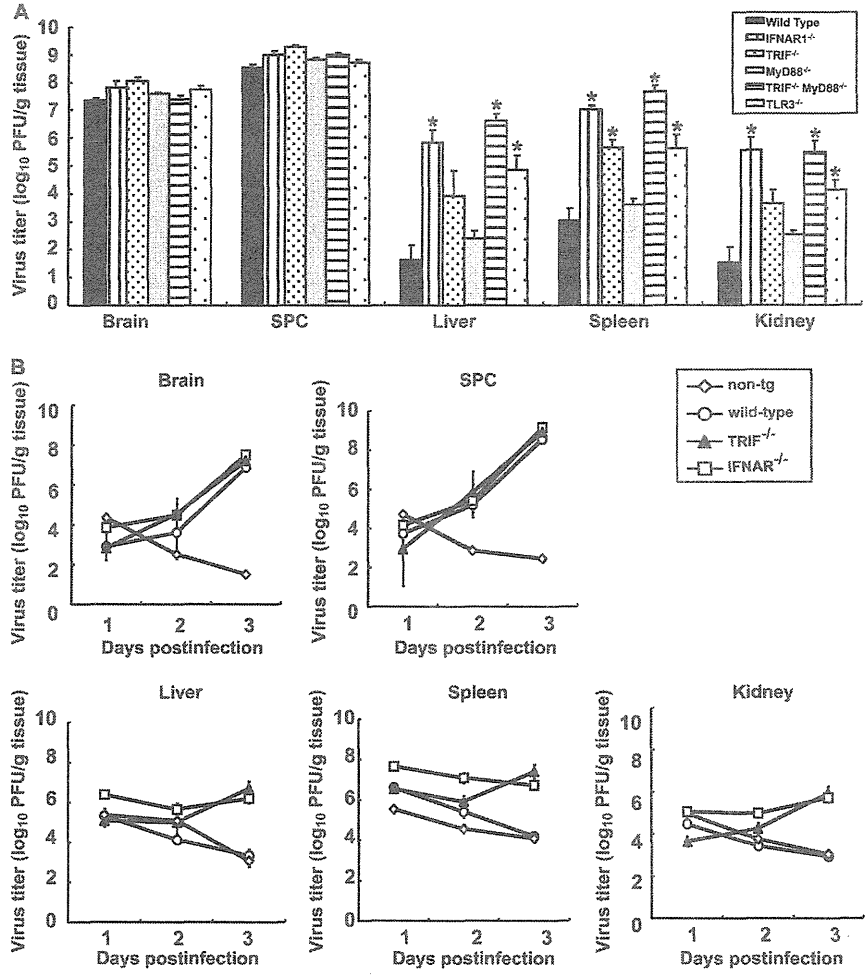

FIG 8 (A) PV replication in TRIF- and MyD88-deficient mice. Wild-type ($n = 4$), $TRIF^{-/-}$ ($n = 4$), $MyD88^{-/-}$ ($n = 6$), $TRIF^{-/-}$ $MyD88^{-/-}$ ($n = 4$), $TLR3^{-/-}$ ($n = 5$), and $IFNAR1^{-/-}$ ($n = 4$) mice were intravenously infected with 10^7 PFU of PV. The infected mice were paralyzed or dead at 3 to 5 days postinfection. The indicated tissues were collected, and viral titers were determined using a plaque assay (*, $P < 0.01$ by t test compared to wild-type mice). (B) PV replication kinetics in TRIF-deficient mice. Nontransgenic mice, wild-type mice, $TRIF^{-/-}$ mice, and $IFNAR1^{-/-}$ mice ($n = 3$) were infected as described above. Tissues were collected daily, and viral titers were determined. The results for nontransgenic (non-tg) mice, wild-type mice, and $IFNAR1^{-/-}$ mice are the same as those in Fig. 4B. SPC, spinal cord.

TABLE 2 PV antigens in TRIF- and MyD88-deficient mice

Organ or tissue	No. of PV antigen-positive mice/no. of mice tested			
	Wild type	$TRIF^{-/-}$	$MyD88^{-/-}$	$TRIF^{-/-}$ $MyD88^{-/-}$
Brain	6/6	8/8	9/9	6/6
Spinal cord	6/6	8/8	9/9	6/6
Heart	0/6	0/8	0/8	0/6
Lung	0/6	0/8	0/8	0/6
Liver	0/6	0/8	0/9	0/6
Kidney	0/6	0/8	2/9	0/5
Spleen	0/6	0/8	0/9	0/6
Pancreas	2/6	0/8	7/9	4/6
Intestine	0/6	0/8	0/9	0/6
Adipose tissue	0/6	2/8	2/9	3/6

mice were compared (Fig. 9). Approximately 25% of the $TRIF^{-/-}$ mice died after infection with 10^2 PFU of PV, and almost all of the mice died after infection with more than 10^3 PFU of PV (Fig. 9A). Approximately 20% and 60% of the $MyD88^{-/-}$ mice died after infection with 10^3 and 10^4 PFU of PV, respectively (Fig. 9B and C). $TRIF^{-/-}$ $MyD88^{-/-}$ mice were the most susceptible. In total, 70% of the mice died after infection with 10^2 PFU of PV (Fig. 9A). The mortality rate of $TRIF^{-/-}$ $MyD88^{-/-}$ mice was very close to that of $IFNAR1^{-/-}$ mice (19). The mortality rate of $TLR3^{-/-}$ mice was similar to that of $TRIF^{-/-}$ mice (Fig. 9D, E, and F). These results suggest that the TRIF-mediated and MyD88-mediated antiviral responses contribute to the host's defense against PV infection and that the TLR3-TRIF-mediated response has the most dominant effect.

DISCUSSION

Each virus infects different cell types and has a characteristic mode of replication. In mammalian hosts, several viral RNA sensors,

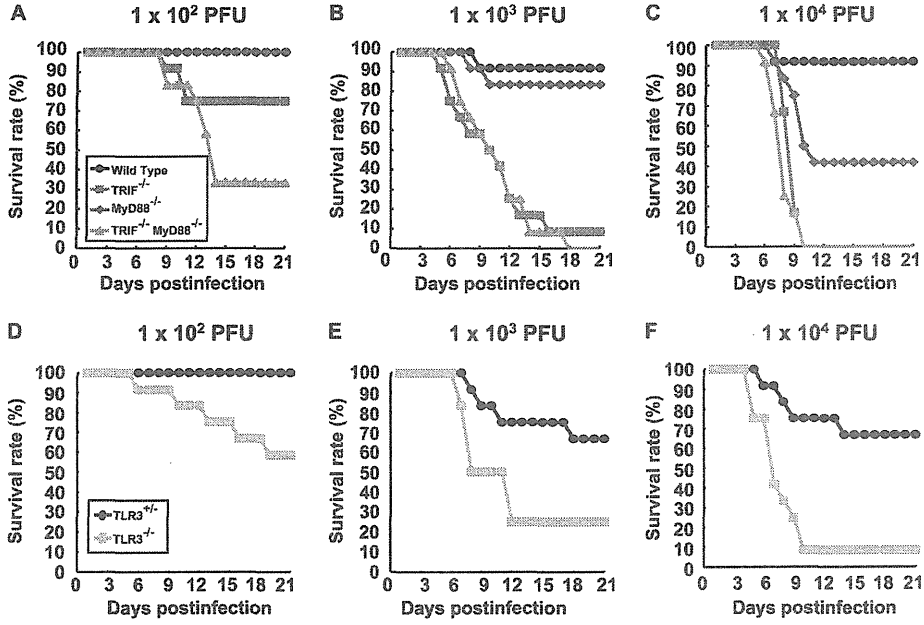

FIG 9 Mortality rates of TRIF-, MyD88-, and TLR3-deficient mice. (A) Wild-type, TRIF$^{-/-}$, MyD88$^{-/-}$, and TRIF$^{-/-}$ MyD88$^{-/-}$ mice (n = 12) were intravenously inoculated with the indicated doses of PV. (B) Littermates of TLR3$^{+/-}$ and TLR3$^{-/-}$ mice (n = 12) were used.

which are expressed in different cell types and recognize different molecular patterns, have evolved to counteract a variety of viruses. In the present study, we demonstrated that the MDA5-, TRIF-, and MyD88-mediated pathways contribute to the recognition of PV infection and that the TLR3-TRIF-mediated pathway plays the most important role in the antiviral response. Since all of the phenotypes shown after PV infection in the TRIF$^{-/-}$ mice and TLR3$^{-/-}$ mice are very similar to each other, we think that the contribution of the TLR3-mediated response is dominant and that of the TLR4-mediated response is negligible.

Previous reports have revealed that IFN is produced efficiently in EMCV-infected fibroblasts in an MDA5-dependent manner and that MDA5 contributes to the induction of serum IFNs and the protection of mice against EMCV (10, 23). Because EMCV belongs to the family *Picornaviridae*, we hypothesized that MDA5 also contributes to IFN induction in response to PV infection. However, the MDA5-dependent pathway did not play a dominant role in the defense against PV infection. Therefore, we speculate that PV uses mechanisms different from those of EMCV to strongly suppress IFN production *in vivo*. Indeed, IFN production in cultured cells in response to PV infection was observed only when the cells were pretreated with a low dose of IFNs. In addition, the amount of IFN produced was much lower than that produced in response to EMCV infection (Fig. 1). This result suggests that IFN induction in infected cells is suppressed and that this PV-mediated effect may be stronger than that of EMCV. Translational shutoff may be one of the reasons for this difference. PV 3A protein causes a change in membrane trafficking that prevents protein secretion and may also contribute to the suppression of IFN production (6). Caspase-dependent cleavage of MDA5 (3) and IPS-1 (39) in PV-infected cells has been reported. Through these possible mechanisms, PV may induce the suppression of IFN production in mice *in vivo*, and the MDA5-mediated pathway does not play an essential role in the host response, unlike in EMCV infection. PV and EMCV seemed to use different strategies to counteract the host innate immune system, even though PV and EMCV belong to the same family. Thus, TLR3 became the sensor that functions most effectively for PV as a result of PV evolution. Although the TLR3-TRIF-mediated pathway plays a dominant role, the fact that significant ISG induction was observed in PV-infected TRIF$^{-/-}$ and TRIF$^{-/-}$ MyD88$^{-/-}$ mice (Fig. 7) suggested that other mechanisms also operate in combination with this pathway.

The viral loads in the nonneural tissues of TLR3- and TRIF-deficient mice were much higher than those in wild-type mice, whereas the viral loads in the CNS were not significantly different in paralyzed mice (Fig. 8). These results suggest that the TLR3-TRIF-mediated pathway inhibits viral replication mainly before viral invasion of the CNS rather than after invasion and that this response plays an important role in preventing the viral invasion of the CNS. In the CNS, replication of PV was not effectively inhibited, even in wild-type mice. This result is consistent with our previous results obtained using IFNAR1$^{-/-}$ mice and suggests that the antivirus response in the CNS is different from that in nonneural tissues upon PV infection (19). The cell tropism of PV may influence the efficiency of the immune response. For example, if PVR is expressed in TLR3-expressing cells, then PV replication would be detected immediately after infection. Alternatively, if PV infection *in vivo* occurs in the vicinity of TLR3-expressing immune cells such as DCs and macrophages, PV-infected cells may readily be captured by TLR3-expressing cells, thereby facilitating efficient cross-priming (27, 44) of PV RNA. PV infects neurons almost exclusively and not other cell types in the CNS. If neurons do not have the ability to induce a strong TLR3-mediated antiviral response upon PV infection, the CNS may be more defective in the innate immune response than nonneural tissues are. This may be one of the reasons why PV replicates preferentially in the CNS. Further studies on PV pathogenesis related to the innate

immune response will make a great contribution to elucidating the mechanisms of PV tissue tropism.

TLR3 recognizes dsRNA. However, the protective role of TLR3 in the response to many RNA viral infections is not clear (9, 29, 43). A previous study has demonstrated that WNV, which is an encephalitis virus belonging to the family *Flaviviridae*, causes more severe encephalitis in mice with intact TLR3 than in TLR3$^{-/-}$ mice. Peripheral WNV infection leads to a breakdown of the blood-brain barrier (BBB) and enhances brain infection in wild-type mice but not in TLR3$^{-/-}$ mice (50). In contrast, a protective role of the TLR3-mediated pathway in PV infection was clearly demonstrated in the present study. PV enters the CNS directly across the BBB via a PVR-independent mechanism (52) and from the neuromuscular junction via retrograde axonal transport (31–33). Because PV originally possesses two entry pathways into the CNS, the generation of a new entry pathway, even if it did occur, might not increase its deteriorative effect.

Interestingly, protective roles of the TLR3-mediated pathway have been reported for group B coxsackievirus (30, 41, 42), human rhinovirus (49), and EMCV (11) infections. Riad et al. (41) demonstrated that TRIF$^{-/-}$ mice showed severe myocarditis after CVB3 infection and IFN-β treatment improved virus control and reduced cardiac inflammation. Richer et al. (42) reported that TLR3$^{-/-}$ mice produced reduced proinflammatory mediators and were unable to control CVB4 replication at the early stages of infection, resulting in severe cardiac damage. They also showed that adoptive transfer of wild-type macrophages into TLR3$^{-/-}$ mice challenged with CVB4 resulted in greater survival, suggesting the importance of the TLR3-mediated pathway in the macrophage. Negishi et al. (30) reported that TLR3$^{-/-}$ mice showed vulnerability to CVB3 and that TLR3 signaling is linked to the activation of the type II IFN system. Since CVB3 does not induce robust type I IFNs, they suggested that the TLR3 type II IFN pathway serves as an "ace in the hole" in infections with such viruses. PV is similar to CVB3 because type I IFN production is low. However, in our preliminary experiments on PV infection in IFN-$\gamma^{-/-}$ PVR-tg mice, type II IFN did not make a significant contribution to the pathogenesis of PV. Taken together, these results suggest a critical role for the TLR3-mediated pathway, but the precise mechanisms leading to host protection are still controversial and the downstream events of TLR3 signaling after picornavirus infection remain to be elucidated.

Because the above-mentioned viruses are picornaviruses, picornavirus RNA may be easily detected by TLR3. There may be a common RNA structure in the genome or in the replication intermediates of these viruses that is detected by TLR3. Alternatively, picornaviral RNA may replicate in a compartment in which TLR3 can easily access the replicating dsRNA. To investigate these hypotheses, identification of the cells responsible for IFN production is an important step. Oshiumi et al. demonstrated that splenic CD8α^+ CD11c$^+$ cells, bone marrow-derived macrophages, and DCs are able to elicit IFN in response to PV infection (35). Further studies using this virus-cell system will elucidate the molecular recognition pattern in the PV genome, the precise mechanism of PV RNA recognition in TLR3-expressing cells, and the roles of these cells in the prevention of PV dissemination in the body.

ACKNOWLEDGMENTS

We thank Takashi Fujita, Mitsutoshi Yoneyama, Hiroki Kato, Masahiro Yamamoto, Satoshi Uematsu, Seiya Yamayoshi, Akira Ainai, Hideki Hasegawa, and Takashi Kawanishi for helpful discussions and technical assistance.

This work was supported, in part, by Grants-in-Aid from the Ministry of Education, Culture, Sports, Science and Technology, Japan (Grants-in-Aid for Scientific Research on Priority Areas no. 21022053), and Grants-in-Aid for Research on Emerging and Re-emerging Infectious Diseases from the Ministry of Health, Labor and Welfare, Japan.

REFERENCES

1. **Akira S, Uematsu S, Takeuchi O.** 2006. Pathogen recognition and innate immunity. Cell 124:783–801.
2. **Alexopoulou L, Holt AC, Medzhitov R, Flavell RA.** 2001. Recognition of double-stranded RNA and activation of NF-kappaB by Toll-like receptor 3. Nature 413:732–738.
3. **Barral PM, et al.** 2007. MDA-5 is cleaved in poliovirus-infected cells. J. Virol. 81:3677–3684.
4. **Bodian D.** 1959. Poliomyelitis: pathogenesis and histopathology, p 479–518. *In*Rivers TM, Horsfall FL, Jr (ed), Viral and rickettsial infections of man, vol 3. J. B. Lippincott, Philadelphia, PA.
5. **Cella M, et al.** 1999. Plasmacytoid monocytes migrate to inflamed lymph nodes and produce large amounts of type I interferon. Nat. Med. 5:919–923.
6. **Choe SS, Dodd DA, Kirkegaard K.** 2005. Inhibition of cellular protein secretion by picornaviral 3A proteins. Virology 337:18–29.
7. **Colonna M, Trinchieri G, Liu YJ.** 2004. Plasmacytoid dendritic cells in immunity. Nat. Immunol. 5:1219–1226.
8. **Diebold SS, Kaisho T, Hemmi H, Akira S, Reis e Sousa C.** 2004. Innate antiviral responses by means of TLR7-mediated recognition of single-stranded RNA. Science 303:1529–1531.
9. **Edelmann KH, et al.** 2004. Does Toll-like receptor 3 play a biological role in virus infections? Virology 322:231–238.
10. **Gitlin L, et al.** 2006. Essential role of mda-5 in type I IFN responses to polyriboinosinic:polyribocytidylic acid and encephalomyocarditis picornavirus. Proc. Natl. Acad. Sci. U. S. A. 103:8459–8464.
11. **Hardarson HS, et al.** 2007. Toll-like receptor 3 is an essential component of the innate stress response in virus-induced cardiac injury. Am. J. Physiol. Heart Circ. Physiol. 292:H251–H258.
12. **Hemmi H, et al.** 2002. Small anti-viral compounds activate immune cells via the TLR7 MyD88-dependent signaling pathway. Nat. Immunol. 3:196–200.
13. **Hoebe K, et al.** 2003. Identification of Lps2 as a key transducer of MyD88-independent TIR signalling. Nature 424:743–748.
14. **Holland JJ.** 1961. Receptor affinities as major determinants of enterovirus tissue tropisms in humans. Virology 15:312–326.
15. **Holland JJ, Mc LL, Syverton JT.** 1959. Mammalian cell-virus relationship. III. Poliovirus production by non-primate cells exposed to poliovirus ribonucleic acid. Proc. Soc. Exp. Biol. Med. 100:843–845.
16. **Holland JJ, McLaren LC, Syverton JT.** 1959. The mammalian cell-virus relationship. IV. Infection of naturally insusceptible cells with enterovirus ribonucleic acid. J. Exp. Med. 110:65–80.
17. **Hornung V, et al.** 2006. 5′-Triphosphate RNA is the ligand for RIG-I. Science 314:994–997.
18. **Hsiung GD, Black FL, Henderson JR.** 1964. Susceptibility of primates to viruses in relation to taxonomic classification, p 1–23. *In*Buettner-Jaenusch J (ed), Evolutionary and genetic biology of primates, vol 2. Academic Press, New York, NY.
19. **Ida-Hosonuma M, et al.** 2005. The alpha/beta interferon response controls tissue tropism and pathogenicity of poliovirus. J. Virol. 79: 4460–4469.
20. **Ida-Hosonuma M, et al.** 2003. Host range of poliovirus is restricted to simians because of a rapid sequence change of the poliovirus receptor gene during evolution. Arch. Virol. 148:29–44.
21. **Kato H, et al.** 2005. Cell type-specific involvement of RIG-I in antiviral response. Immunity 23:19–28.
22. **Kato H, et al.** 2008. Length-dependent recognition of double-stranded ribonucleic acids by retinoic acid-inducible gene-I and melanoma differentiation-associated gene 5. J. Exp. Med. 205:1601–1610.
23. **Kato H, et al.** 2006. Differential roles of MDA5 and RIG-I helicases in the recognition of RNA viruses. Nature 441:101–105.
24. **Koike S, et al.** 1992. A second gene for the African green monkey poliovirus receptor that has no putative N-glycosylation site in the functional N-terminal immunoglobulin-like domain. J. Virol. 66:7059–7066.

25. **Koike S, Nomoto A.** 2010. Poliomyelitis, p 339–351. *In*Ehrenfeld E, Domingo E, Roos RP (ed), The picornaviruses. ASM Press, Washington, DC.
26. **Koike S, et al.** 1991. Transgenic mice susceptible to poliovirus. Proc. Natl. Acad. Sci. U. S. A. **88**:951–955.
27. **Kramer M, et al.** 2008. Phagocytosis of picornavirus-infected cells induces an RNA-dependent antiviral state in human dendritic cells. J. Virol. 82:2930–2937.
28. **Matsumoto M, et al.** 2003. Subcellular localization of Toll-like receptor 3 in human dendritic cells. J. Immunol. 171:3154–3162.
29. **Matsumoto M, Oshiumi H, Seya T.** 2011. Antiviral responses induced by the TLR3 pathway. Rev. Med. Virol. **21**:67–77.
30. **Negishi H, et al.** 2008. A critical link between Toll-like receptor 3 and type II interferon signaling pathways in antiviral innate immunity. Proc. Natl. Acad. Sci. U. S. A. **105**:20446–20451.
31. **Ohka S, et al.** 2004. Receptor (CD155)-dependent endocytosis of poliovirus and retrograde axonal transport of the endosome. J. Virol. **78**: 7186–7198.
32. **Ohka S, et al.** 2009. Receptor-dependent and -independent axonal retrograde transport of poliovirus in motor neurons. J. Virol. **83**:4995–5004.
33. **Ohka S, Yang WX, Terada E, Iwasaki K, Nomoto A.** 1998. Retrograde transport of intact poliovirus through the axon via the fast transport system. Virology **250**:67–75.
34. **Oshiumi H, Matsumoto M, Funami K, Akazawa T, Seya T.** 2003. TICAM-1, an adaptor molecule that participates in Toll-like receptor 3-mediated interferon-beta induction. Nat. Immunol. 4:161–167.
35. **Oshiumi H, et al.** 12 October 2011, posting date. The TLR3-TICAM-1 pathway is mandatory for innate immune responses to poliovirus infection. J. Immunol. [Epub ahead of print.] doi:10.4049/jimmunol.1101503.
36. **Pichlmair A, et al.** 2006. RIG-I-mediated antiviral responses to single-stranded RNA bearing 5′-phosphates. Science **314**:997–1001.
37. **Pichlmair A, et al.** 2009. Activation of MDA5 requires higher-order RNA structures generated during virus infection. J. Virol. **83**:10761–10769.
38. **Racaniello VR.** 2007. Picornaviridae: the viruses and their replication, p 795–838. *In*Knipe DM, Howley PM (ed), Fields virology, 5th ed. Lippincott Williams & Wilkins, Philadelphia, PA.
39. **Rebsamen M, Meylan E, Curran J, Tschopp J.** 2008. The antiviral adaptor proteins Cardif and Trif are processed and inactivated by caspases. Cell Death Differ. 15:1804–1811.
40. **Ren RB, Costantini F, Gorgacz EJ, Lee JJ, Racaniello VR.** 1990. Transgenic mice expressing a human poliovirus receptor: a new model for poliomyelitis. Cell **63**:353–362.
41. **Riad A, et al.** 2011. TRIF is a critical survival factor in viral cardiomyopathy. J. Immunol. **186**:2561–2570.
42. **Richer MJ, Lavallee DJ, Shanina I, Horwitz MS.** 2009. Toll-like receptor 3 signaling on macrophages is required for survival following coxsackievirus B4 infection. PLoS One **4**:e4127.
43. **Schröder M, Bowie AG.** 2005. TLR3 in antiviral immunity: key player or bystander? Trends Immunol. **26**:462–468.
44. **Schulz O, et al.** 2005. Toll-like receptor 3 promotes cross-priming to virus-infected cells. Nature 433:887–892.
45. **Shiroki K, et al.** 1995. A new *cis*-acting element for RNA replication within the 5′ noncoding region of poliovirus type 1 RNA. J. Virol. 69: 6825–6832.
46. **Takeuchi O, Akira S.** 2009. Innate immunity to virus infection. Immunol. Rev. **227**:75–86.
47. **Takeuchi O, Akira S.** 2008. MDA5/RIG-I and virus recognition. Curr. Opin. Immunol. **20**:17–22.
48. **Takeuchi O, Akira S.** 2007. Recognition of viruses by innate immunity. Immunol. Rev. **220**:214–224.
49. **Wang Q, et al.** 2009. Role of double-stranded RNA pattern recognition receptors in rhinovirus-induced airway epithelial cell responses. J. Immunol. 183:6989–6997.
50. **Wang T, et al.** 2004. Toll-like receptor 3 mediates West Nile virus entry into the brain causing lethal encephalitis. Nat. Med. **10**:1366–1373.
51. **Yamamoto M, et al.** 2003. Role of adaptor TRIF in the MyD88-independent Toll-like receptor signaling pathway. Science **301**:640–643.
52. **Yang WX, et al.** 1997. Efficient delivery of circulating poliovirus to the central nervous system independently of poliovirus receptor. Virology **229**:421–428.
53. **Yoneyama M, et al.** 2004. The RNA helicase RIG-I has an essential function in double-stranded RNA-induced innate antiviral responses. Nat. Immunol. 5:730–737.
54. **Yoshikawa T, et al.** 2006. Role of the alpha/beta interferon response in the acquisition of susceptibility to poliovirus by kidney cells in culture. J. Virol. **80**:4313–4325.
55. **Yousefi S, Escobar MR, Gouldin CW.** 1985. A practical cytopathic effect/dye-uptake interferon assay for routine use in the clinical laboratory. Am. J. Clin. Pathol. **83**:735–740.

RESEARCH PAPER

OncoImmunology 1:5, 581-592; August 2012; © 2012 Landes Bioscience

Cross-priming for antitumor CTL induced by soluble Ag + polyI:C depends on the TICAM-1 pathway in mouse CD11c$^+$/CD8α$^+$ dendritic cells

Masahiro Azuma, Takashi Ebihara,† Hiroyuki Oshiumi, Misako Matsumoto and Tsukasa Seya*

Department of Microbiology and Immunology; Hokkaido University Graduate School of Medicine; Sapporo, Japan

†Current affiliation: Howard Hughes Medical Institute; Washington University School of Medicine; St. Louis, MO USA

Keywords: cross-presentation, dendritic cell, TLR3, TICAM-1 (TRIF), tumoricidal CTL

Abbreviations: APC, antigen-presenting cells; CTL, cytotoxic T lymphocytes; DAMP, damage-associated molecular pattern; DC, dendritic cells; IFN, interferon; IPS-1, IFNβ promoter stimulator-1; MDA5, melanoma differentiation associated gene 5; Mf, macrophages; NK, natural killer; OVA, ovalbumin; PAMP, pathogen-associated molecular pattern; PRR, pattern-recognition receptors; PV, poliovirus; RIG-I, retinoic acid inducible gene-1; SL8, an OVA tetramer; TICAM-1, Toll-IL-1 receptor homology domain-containing molecule-1; TLR, Toll-like receptor; WT, wild-type

PolyI:C is a nucleotide pattern molecule that induces cross-presentation of foreign Ag in myeloid dendritic cells (DC) and MHC Class I-dependent proliferation of cytotoxic T lymphocytes (CTL). DC (BM or spleen CD8α$^+$) have sensors for dsRNA including polyI:C to signal facilitating cross-presentation. Endosomal TLR3 and cytoplasmic RIG-I/MDA5 are reportedly responsible for polyI:C sensing and presumed to deliver signal for cross-presentation via TICAM-1 (TRIF) and IPS-1 (MAVS, Cardif, VISA) adaptors, respectively. In fact, when tumor-associated Ag (TAA) was simultaneously taken up with polyI:C in DC, the DC cross-primed CTL specific to the TAA in a syngenic mouse model. Here we tested which of the TICAM-1 or IPS-1 pathway participate in cross-presentation of tumor-associated soluble Ag and retardation of tumor growth in the setting with a syngeneic tumor implant system, EG7/C57BL6, and exogenously challenged soluble Ag (EG7 lysate) and polyI:C. When EG7 lysate and polyI:C were subcutaneously injected in tumor-bearing mice, EG7 tumor growth retardation was observed in wild-type and to a lesser extent IPS-1$^{-/-}$ mice, but not TICAM-1$^{-/-}$ mice. IRF-3/7 were essential but IPS-1 and type I IFN were minimally involved in the polyI:C-mediated CTL proliferation. Although both TICAM-1 and IPS-1 contributed to CD86/CD40 upregulation in CD8α$^+$ DC, H2K^b-SL8 tetramer and OT-1 proliferation assays indicated that OVA-recognizing CD8 T cells predominantly proliferated in vivo through TICAM-1 and CD8α$^+$ DC is crucial in ex vivo analysis. Ultimately, tumor regresses > 8 d post polyI:C administration. The results infer that soluble tumor Ag induces tumor growth retardation, i.e., therapeutic potential, if the TICAM-1 signal coincidentally occurs in CD8α$^+$ DC around the tumor.

Introduction

Cytotoxic T lymphocytes (CTL) and natural killer (NK) cells are two major effectors for antitumor cellular immunity. These effectors are driven through activation of dendritic cells (DC) and/or macrophages (Mf), which is mediated by pattern-recognition receptors (PRRs) for the recognition of microbial patterns.[1,2] Antigen (Ag) presentation and upregulation of NK cell-activating ligands are major events induced in DC/Mf in response to PRRs, which link to evoking CTL- and NK-antitumor immunity, respectively. The immune-potentiating function of specific components of the classical adjuvants are largely attributable to the ligand activity of PRRs (CpG DNA/TLR9, polyI:C/TLR3, monophosphoryl lipid (MPL) A/TLR4, Pam2/TLR2, etc.).[3] That is, the DC/Mf competent to drive effectors are generated through PRR signal in inflammatory nest where affected cells and recruited immune cells encounter exogenous or endogenous PRR ligands. Since studying the functional properties of PRRs in tumor immunity is on the way using a variety of possible ligands and cell biological analyses, immune responses reflecting the total adjuvant potential around Ag-presenting cells (APC) in local inflammatory nests are not always elucidated even in mice.

RNA-sensing PRR pathways, including TLR3-TICAM-1, TLR7-MyD88 and RIG-I/MDA5-IPS-1 participate in driving Type I IFN induction and cellular immunity in DC subsets.[1,4,5] Type I IFN and the IFNAR pathway in DC and other cells reportedly evoke and amplify T cell immunity.[5,6] TLR7 resides exclusively in plasmacytoid DC[7] whereas TLR3 mainly exists in

*Correspondence to: Tsukasa Seya; Email: seya-tu@pop.med.hokudai.ac.jp
Submitted: 02/04/12; Revised: 03/02/12; Accepted: 03/02/12
http://dx.doi.org/10.4161/onci.19893

myeloid DC/Mf and epithelial cells.[8] They are localized on the membrane of the endosome and deliver the signal via their adaptors, MyD88 and TICAM-1.[7,8] RIG-I and MDA5 are ubiquitously distributed to a variety of mouse cells and signal the presence of cytoplasmic viral products through IPS-1.[9] Thus, TLR3 and RIG-I/MDA5 are candidates associated with DC maturation to drive effector cells.[10] Indeed, viral dsRNA analog, polyI:C, is a representative ligand for TLR3 and MDA5 and induces polyI:C-mediated DC-NK reciprocal activation.[11,12] These are also true in human DC.[13]

The point of this study is by which pathway antitumor CTL are induced for tumor regression in a mouse tumor-implant model. It has been postulated that DC present exogenous tumor Ag to the MHC Class I-restricted Ag-presentation pathway and proliferate CD8 T cells specific to the extrinsic Ag. When tumor cells provide soluble and insoluble exogenous Ag, this Class I Ag presentation occurs mostly TAP/proteasome-dependent, suggesting the pathway partly sharing with that for endogenous Ag presentation. This DC's ability to deliver exogenous Ag to the pathway for MHC Class I-restricted Ag presentation has been described as cross-presentation.[14] DC cross-presentation leads to the cross-priming and proliferation of Ag-specific CD8 T cells in vivo and in vitro.[14-18] A variety of PAMP[15,16] and intrinsic DAMP[17] as well as other factors including Type I IFN,[5,18] $CD4^+$ T cells[19] and NKT cells[20] augment cross-priming in tumor-bearing mice. However, by what molecular mechanism polyI:C enhances CTL induction in tumor-bearing mice remains largely unsettled.

Here, we made an EG7 tumor-implant mouse system and treated the mice with s.c.-injected ovalbumin (OVA)-containing cell lysates (Ag) and polyI:C. Spleen $CD8\alpha^+$ DC turn CTL-inducible when stimulated with Ag and polyI:C. In either case of s.c., i.p., or i.v. injection of polyI:C, the TLR3/TICAM-1 pathway predominantly participates in $CD8\alpha^+$ DC cross-priming and antitumor CTL induction. Earlier studies using non-tumor models, suggested that both TLR3 and MDA5 appeared to participate in polyI:C-dependent CTL induction.[21] TLR3 is predominantly involved in primary Ag response and Th1 skewing,[22] while MDA5 participates in secondary Ag response.[23] Importance of TLR3 in induction of cross-priming was first suggested by Schulz et al., who used OVA/polyI:C-loaded or virus-infected xenogenic (Vero) cells and mouse DC.[16] Here we demonstrate that the antitumor polyI:C activity is sustained by the TICAM-1 pathway in any route of injection in tumor-implant mice: antitumor CTL responses are mostly abrogated in TICAM-$1^{-/-}$ but not IPS-$1^{-/-}$ mice.

Results

Properties of EG7 tumor with high MHC in tumor-loading mice. The properties of the EG7 line we used are consistent with those reported previously.[24,25] It expressed high MHC Class I (H2-Kb) and no Qa-1b or Rae-1 (**Fig. S1**). The expression levels of these proteins were barely changed before and after implantation of EG7 cells into mice. Cell viability was not affected by in vitro stimulation with polyI:C only (**Fig. S1B**). However, a batch-to-batch difference of cell viability may have affected the rate of tumor growth in each mouse tumor-implant experiment.

$CD8^+$ T cells are responsible for tumor retardation by polyI:C. EG7 cells (2×10^6) were inoculated into the back of C57BL/6 (WT), and the indicated reagents were subcutaneously (s.c.) injected around the EG7 tumor (**Fig. 1A**). Growth retardation of tumor was observed by treatment with polyI:C or polyI:C plus EG7 lysate (**Fig. 1A**). EG7 lysate only had no effect on tumor regression. When $CD8\beta^+$ T cells were depleted before EG7 lysate/polyI:C treatment, polyI:C-mediated tumor growth suppression was cancelled (**Fig. 1A**), suggesting the participation of CD8 T cells in tumor growth suppression. The therapeutic potential of polyI:C appeared to be more reproducible in the presence of EG7 lysate than in the absence, judged from the increases of activated $CD8^+$ T cells (**Fig. 1B**) and cytotoxic activity (**Fig. 1C**) of LN T cells isolated from the mice sacrificed after the last therapy. Yet, the EG7 Ag could be more or less supplied from the implant tumor. $NK1.1^+$ cells did not participate in this EG7 tumor regression in this setting (data not shown).

Since EG7 lysate contains OVA, OVA-specific T cells in draining LN and spleen of the WT mice were counted by tetramer assay after the last therapy (**Fig. S2A and B**). The numbers of tetramer-positive cells were prominently increased in LN and spleen in mice with EG7 lysate and polyI:C. We confirmed the importance of simultaneous administration of Ag plus polyI:C for OVA-specific CTL induction as in **Figure S2C**, where pure Ag (OVA) was used instead of EG7 lysate for immunotherapy. The polyI:C adjuvant function appeared to be more efficient in the mixture of pure Ag than in polyI:C alone. Tumor regression (**Fig. S2C**) and OVA-specific CTL induction (**Fig. S2D**) were clearly observed in this additional experiment. To obtain reproducible data, we employed the EG7 lysate/polyI:C combination therapy as follows.

IFN-inducing pathways are involved in PolyI:C-derived EG7 growth retardation. We next inoculated EG7 cells (2×10^6) into the back of C57BL/6 (WT), TICAM-$1^{-/-}$, IPS-$1^{-/-}$, or TICAM-1/IPS-1 double-deficient (DKO) mice (**Fig. 2**). We s.c. administered EG7 lysate with or without polyI:C around the tumor. The EG7 lysate was the soluble fraction of EG7 which removed insoluble debris by centrifugation. The EG7 lysate contained unprecipitated micro-debris and soluble Ag. No other emulsified reagent was added for immunization. Thus, the adjuvant function of polyI:C per se is reflected in the tumor growth, although polyI:C had to be injected into mice twice a week. Retardation of tumor growth was observed > 8 d after immunization with EG7 lysate + polyI:C in WT mice, though no growth retardation without polyI:C (**Fig. 2A**). The polyI:C-mediated tumor growth suppression was largely abrogated in TICAM-$1^{-/-}$ (**Fig. 2B**) and to a lesser extent in IPS-$1^{-/-}$ mice (Fig. 2C), and completely in TICAM-1/IPS-1 DKO mice (Fig. 2D). Hence, TICAM-1 plays an important role in inducing polyI:C-mediated tumor growth retardation in the s.c. setting we employed.

CD8 T cell activation induced by the TICAM-1 pathway. CD8 T cell activation in the inguinal LN was tested with polyI:C + EG7 lysate in EG7 tumor-bearing mice using CD69 as

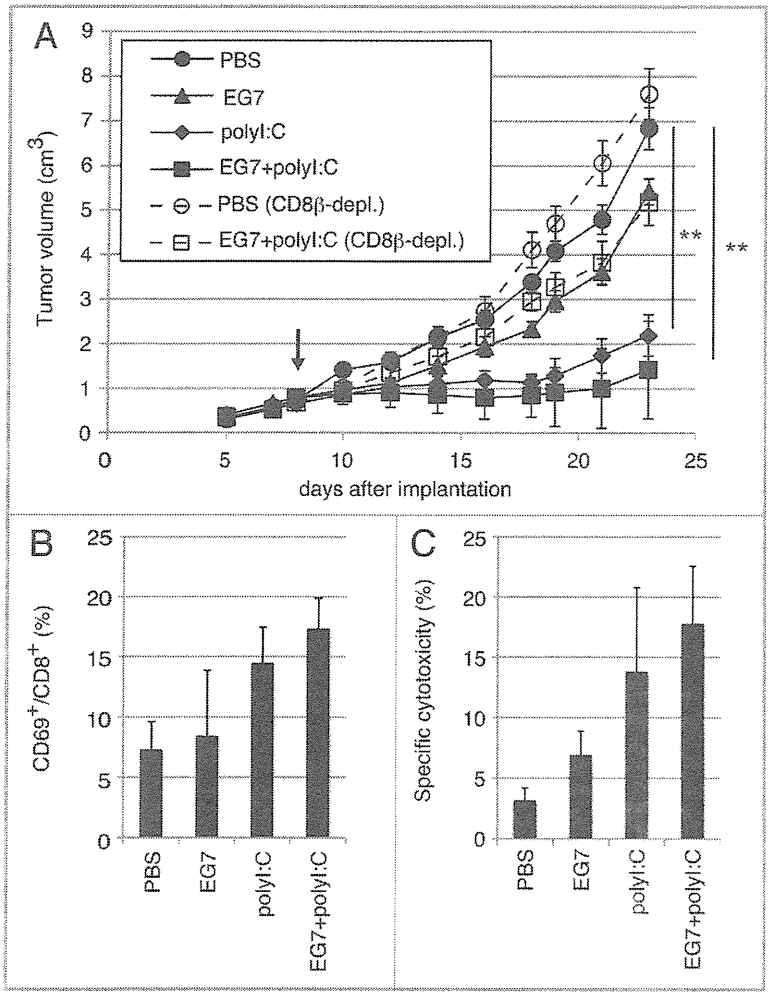

Figure 1. PolyI:C induces CTL-mediated tumor regression. (A) WT mice were challenged with EG7 cells and were treated with PBS (●), EG7 lysates (▲), polyI:C (◆) and EG7 lysates + polyI:C (■). The adjuvant therapy was started at the time indicated by the arrow and the indicated reagents injected twice per week. One of the two PBS groups (○) and one of the two EG7 lysates + polyI:C groups (□) were treated with anti-CD8β ascites in order to deplete $CD8^+$ T cells once a week. Each group had 3–5 mice. (B) Draining inguinal LNs were harvested 24 h after the last treatment and the proportion of CD69-expressing $CD8^+$ cells were counted. (C) LN cells were co-cultured with MMC-treated EG7 cells for 3 d and subjected to ^{51}Cr release assay to evaluate CTL activity. E/T = 50. All error bars used in this figure show ± SEM. Data are representative of two independent experiments. One-way analysis of variance (ANOVA) with Bonferroni's test was performed to analyze statistical significance. **, $p < 0.01$.

an activating marker. Twenty-four hours after the last polyI:C + EG7 sec.c. treatment, cells were harvested from the LN excised (Fig. 3A). FACS profiles of total cells from each mouse group are shown in Fig. S3. By combination therapy with EG7 lysate and polyI:C, T cells were activated in WT and IPS-$1^{-/-}$ mice, but the proportion of CD8 T cells was not affected by the therapy (Fig. S4A). Under the same conditions, T cells were barely activated in TICAM-$1^{-/-}$ mice in response to polyI:C (Fig. 3A). The proportion of $CD69^+$ cells are indicated in Figure 3B. IL-2 (Fig. 3C) and IFNγ (Fig. S4B) were highly induced in the WT and IPS-$1^{-/-}$ LN cells, while they were not induced in TICAM-$1^{-/-}$ or DKO cells. IFNγ levels were upregulated only in polyI:C-treated tumor-bearing mice, although the WT > IPS-$1^{-/-}$ profile for IFNγ production was reproducibly observed (Fig. S4B).

In vivo proliferation of CD8 T cells judged by tetramer assay and IFNγ induction. We next tested whether i.p. injection of polyI:C plus OVA induces CTL proliferation. PolyI:C and OVA were i.p. injected into mice and the polyI:C-dependent cross-priming of CD8 T cells were examined using the OVA tetramer assay. OVA-specific CD8 T cells were clonally proliferated in WT and IPS-$1^{-/-}$ mice, but not in TICAM-1/IPS-1 DKO and IRF-$3/7^{-/-}$ mice (Fig. 4A). Proliferation of OVA-specific CD8 T cells were severely suppressed in TICAM-$1^{-/-}$ mice (Fig. 4A), suggesting that polyI:C-mediated cross-priming of CD8 T cells largely depends on the TICAM-1 pathway followed by IRF-3/7 activation in the i.p. route. The results were reproduced in additional experiments using more mice (Fig. 4B) and TLR$3^{-/-}$ mice (Fig. S5A and B). The polyI:C cytokine response, where IFNα is IPS-1-dependent while IL-12p40 is TICAM-1-dependent, was also confirmed in serum level by polyI:C i.p. injection (Fig. S5E). Specific induction of IFNγ (Fig. 4C) was also observed in parallel with the results of Figure 4A.

Whether or not i.v. injection of polyI:C plus OVA induces Ag-specific CTL and cytotoxicity was next checked. OVA-specific OT-1 proliferation and cytotoxicity (Fig. 4D and E) were observed in in vivo analyses of WT and IPS-$1^{-/-}$ CD8 T cells but not of TICAM-$1^{-/-}$, TICAM-1/IPS-1 DKO, and IRF-$3/7^{-/-}$ mice in the i.v. setting.

Since TICAM-1 is the adaptor for TLR3 as well as cytoplasmic helicases,[24] we confirmed the level of cross-priming being decreased in TLR$3^{-/-}$ mice and an expected result was obtained (Fig. S5A and B). Furthermore, in IFNAR$^{-/-}$ mice, OVA-specific CTL induction was slightly reduced compared with that in WT mice, but higher than in TICAM-$1^{-/-}$ mice (Fig. S5C and D). Hence, in vivo cross-presentation induced by polyI:C mostly depends on the TLR3-TICAM-1 pathway followed by transcriptional regulation by IRF-3/7 in any administration route, and is further promoted by Type I IFN presumably produced by the stromal cells through the IPS-1 pathway.[26]

IPS-1 induces DC maturation but not cross-priming in vivo. Spleen DC maturation by i.v.-injected polyI:C was tested ex vivo using $CD8\alpha^+$ DC and $CD8\alpha^-$ DC isolated from WT or KO mice with no tumor as indicated in Figure 5A. The maturation markers CD86 and CD40 were upregulated on both $CD8\alpha^+$ and $CD8\alpha^-$

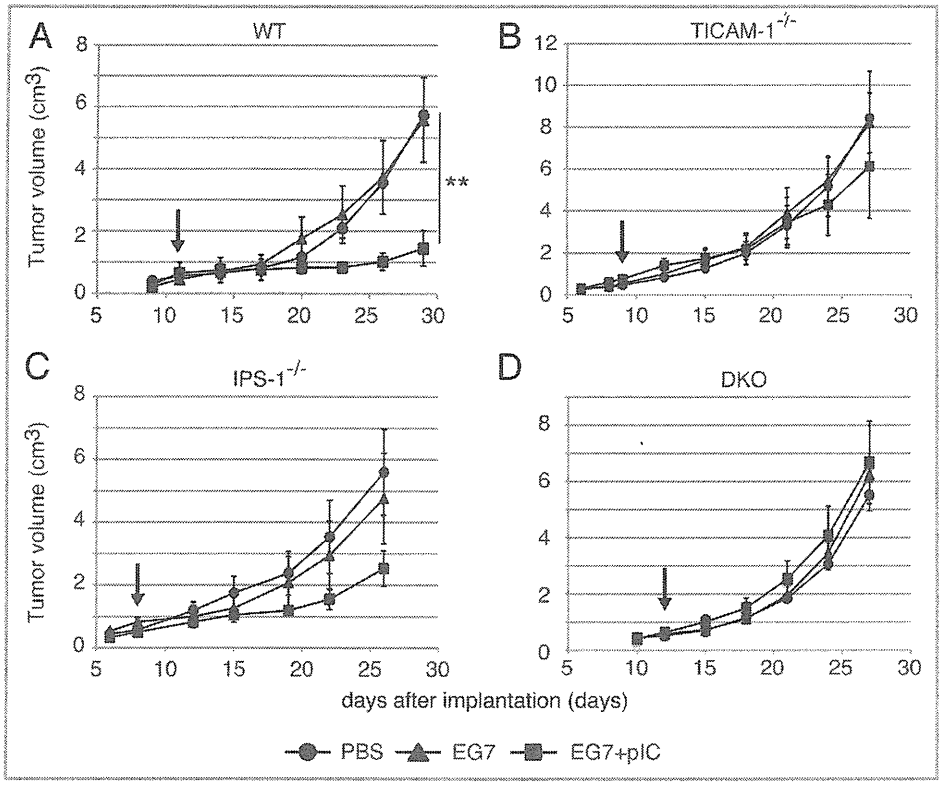

Figure 2. PolyI:C-induced tumor retardation is dependent on the TICAM-1 pathway. Antitumor effect of polyI:C on various KO mice were evaluated by using in vivo mouse tumor implant model. EG7 cells were inoculated to WT (A), TICAM-1$^{-/-}$ (B), IPS-1$^{-/-}$ (C) and DKO mice (D) on day 0. PBS (●), EG7 lysates (▲) or EG7 lysates + polyI:C (■) were s.c. administered around the tumor. The adjuvant therapies were started at the time indicated by the arrows and injected twice per week. Each group have 3–4 mice and error bar shows ± SEM. Data are representative of two independent experiments. **, $p < 0.01$

DC from WT mice when they were stimulated with OVA and polyI:C. Treatment of DC with OVA only did not induce upregulation of CD86 and CD40. Although the expression levels of CD86 and CD40 were a little less in CD8α$^+$ and CD8α$^-$ DC from TICAM-1$^{-/-}$ or IPS-1$^{-/-}$ mice than those from WT mice, both CD86 and CD40 were sufficiently upregulated even in the abrogation of either one pathway in polyI:C-injected mice. The CD86 and CD40 shifts were completely abolished in DKO mice (**Fig. 5A**). Thus, the TICAM-1 pathway participates in both potent co-stimulation and cross-priming, while the IPS-1 pathway mainly participates only in integral co-stimulation in myeloid DC.

We next assessed in vitro proliferation of OT-1 cells. CD8α$^+$ and CD8α$^-$ DC were prepared from PBS, polyI:C, OVA and OVA/polyI:C-treated mice, and mixed in vitro with CFSE-labeled OT-1 cells. WT, TICAM-1$^{-/-}$ and IPS-1$^{-/-}$ mice were used for this study. OT-1 proliferation was observed with CD8α$^+$ DC but not CD8α$^-$ DC when OVA + polyI:C was injected (**Fig. 5B**). Furthermore, the OT-1 proliferation barely occurred in the mixture containing TICAM-1$^{-/-}$ CD8α$^+$ DC. Thus, OT-1 proliferation is triggered by the TICAM-1 pathway in CD8α$^+$ DC. Again, IPS-1 had almost no effect on OT-1 proliferation with CD8α$^+$ DC in this setting. In the mixture, IFNγ was produced in the supernatants of WT and IPS-1$^{-/-}$ CD8α$^+$ DC but not TICAM-1$^{-/-}$ DC by stimulation with OVA + polyI:C (**Fig. 5C**). No IFNγ was produced in the supernatants of CD8α$^-$ DC even from WT mice, which results are in parallel with those of OT-1 proliferation. In any case irrespective of tumor-bearing or not, Ag, polyI:C and the TICAM-1 pathway are mandatory for CD8α$^+$ DC to cross-prime and proliferate OVA-specific CD8 T cells.

We checked the TICAM-1- or IPS-1-specific gene expressions related to Type I IFN and MHC Class I presentation using genechip and qPCR (**Fig. S6**). PolyI:C-mediated upregulation of *Tap1*, *Tap2* and *Tapbp* messages diminished in TICAM-1$^{-/-}$ BMDC (**Fig. S6A**). The levels of these genes were hardly affected in IPS-1$^{-/-}$ BMDC (data not shown). PolyI:C-mediated upregulation was observed with MDA5 (*Ifih1*) in CD8α$^-$ and CD8α$^+$ DCs (**Fig. S6B**). Surprisingly, other factors including TLR3, TICAM-1 and MAVS messages were all downregulated in response to polyI:C in CD8α$^+$ DC (**Fig. S6B**), for the reason as yet unknown.

Effect of TLR3-mediated IFN-inducing pathway on anti-tumor CTL induction. PolyI:C is a dsRNA analog capable of incorporating into the endosome and cytoplasm by exogenous administration in vitro.[27,28] However, no evidence has been proposed that polyI:C is internalized into the endosome of

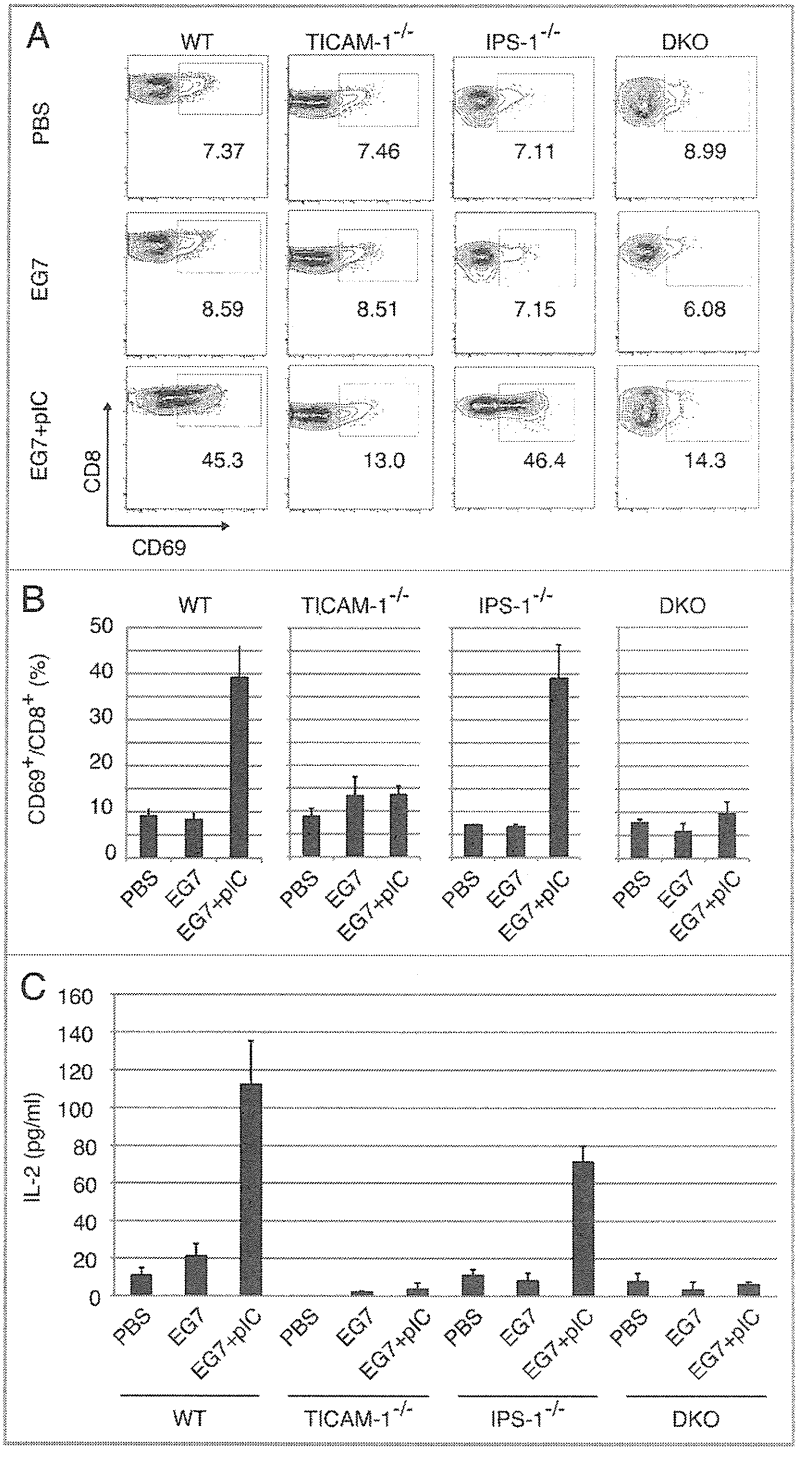

Figure 3. CD8 T cells in the draining LNs are activated through the TICAM-1 pathway by polyI:C. Draining inguinal LNs were harvested from tumor-bearing mice 24 h after the last treatment. LN cells were stained with CD3ε, CD8α and CD69, and the cells gated on $CD3\varepsilon^{+}CD8\alpha^{+}$ are shown (A). Spleen cells in each group of mice were stained separately, the CD8 levels in gated cells being variably distributed in FACS analyses. The average frequency of activated CD8 T cells defined by CD69 expression is shown (B). Alternatively, LN cells from the indicated mice were cultured for further 3 d in vitro and IL-2 production was measured by CBA assay (C).

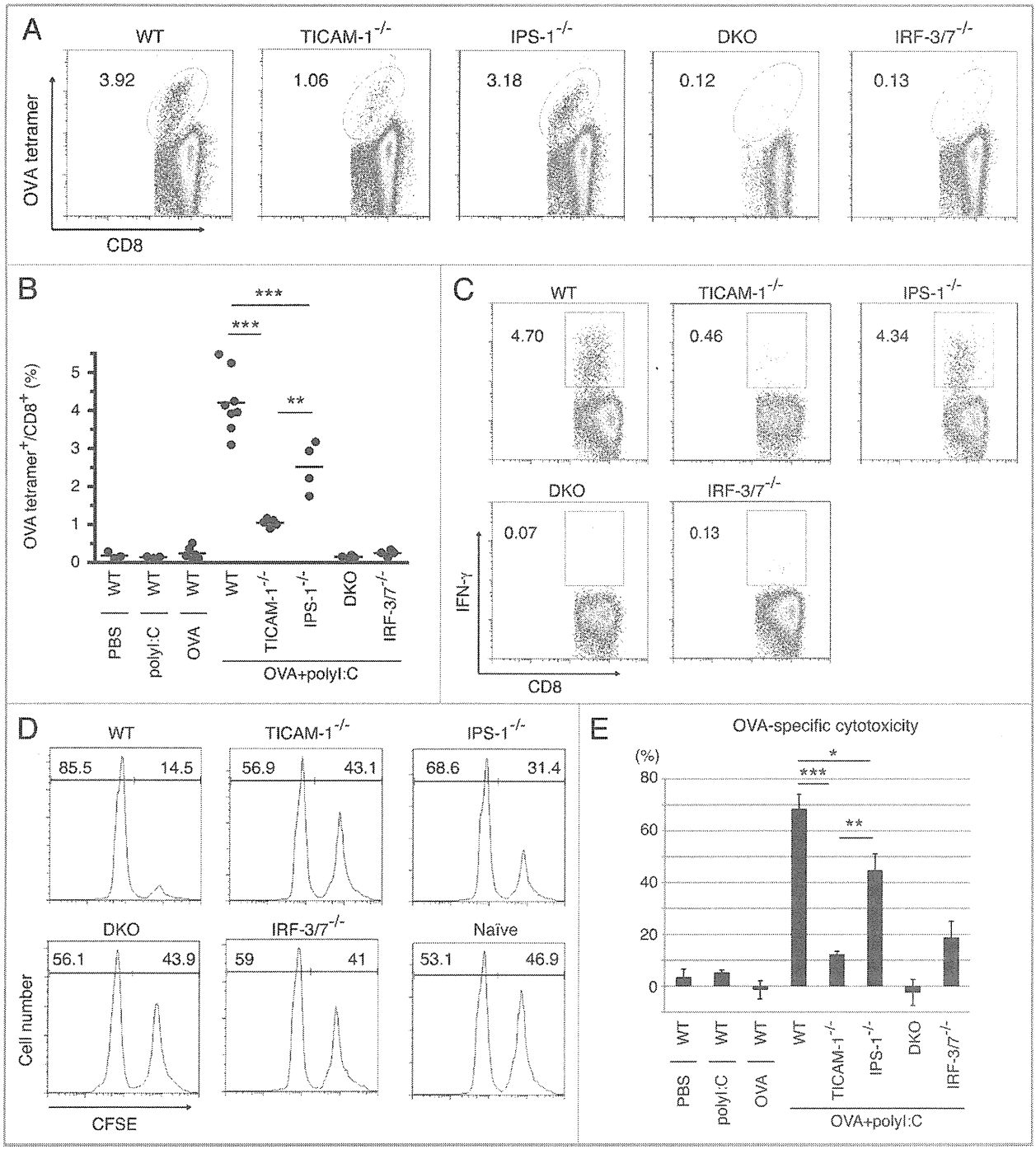

Figure 4. TICAM-1 and IRF-3/7 are essential for polyI:C-induced antigen-specific CTL expansion. WT, TICAM-1$^{-/-}$, IPS-1$^{-/-}$, TICAM-1/IPS-1 DKO and IRF-3/7$^{-/-}$ mice were i.p. administered with the combination of OVA and polyI:C. After 7days, splenocytes were harvested and stained with CD8α and OVA tetramer (A). The average percentages of OVA-specific CTL are shown (B). Alternatively, splenocytes were cultured in vitro in the presence of SL8 for 8 h and IFNγ production was measured by intracellular cytokine staining (C). To assess the killing activity, in vivo CTL assay was performed. The combinations of OVA and polyI:C were administered i.v. to each group of mice and 5 d later, cytotoxicity was measured (D). The data shown are collaborate or representative of at least three independent experiments. One-way analysis of variance (ANOVA) with Bonferroni's test was performed to analyze statistical significance. *, $p < 0.05$; **, $p < 0.01$; ***, $p < 0.001$.

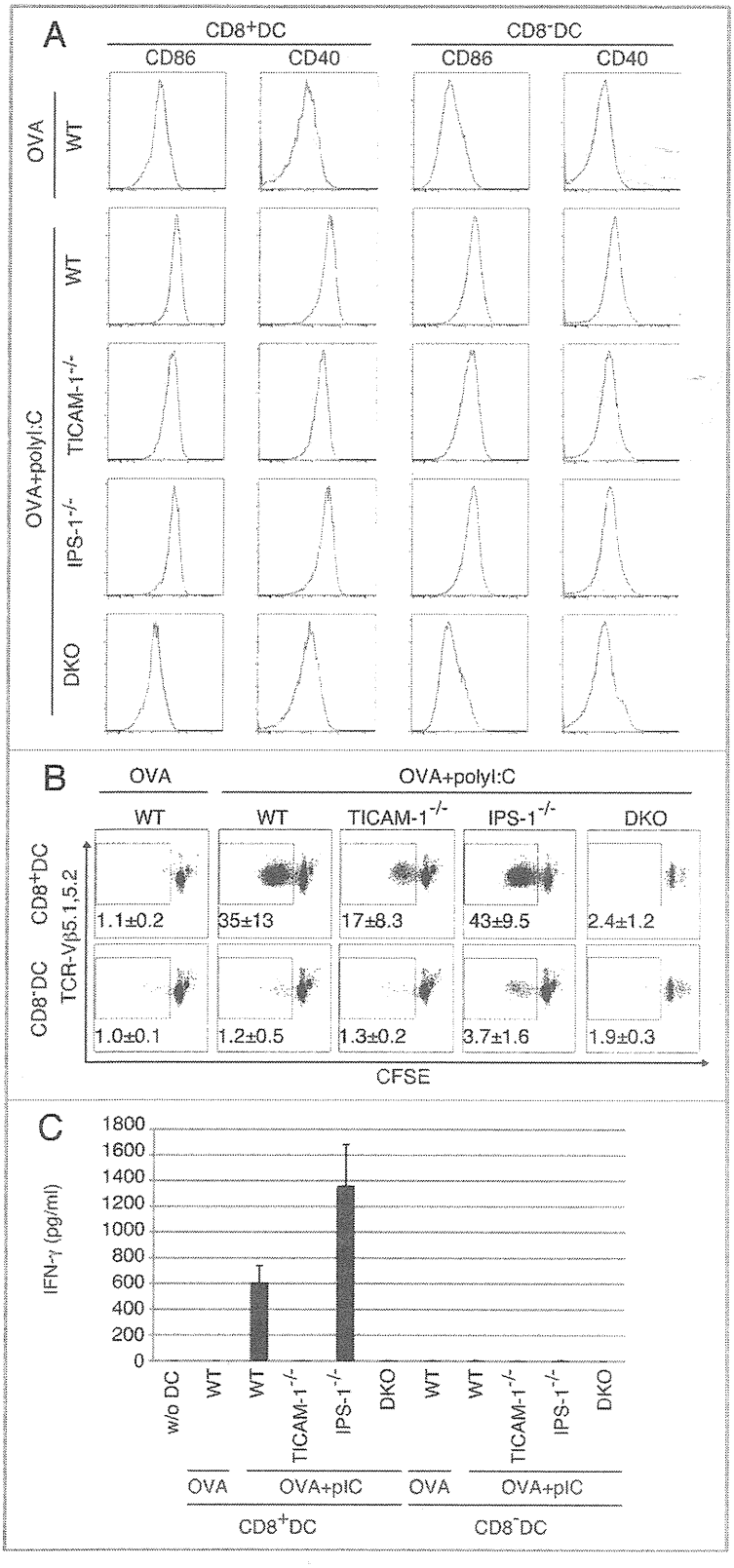

Figure 5. TICAM-1 in CD8α⁺ DC is more important than IPS-1 in polyI:C-induced cross-priming. OVA and polyI:C were administered i.v. and 4 h later, CD8α⁺ and CD8α⁻ DC were isolated from the spleen. CD86 and CD40 expressions were determined by FACS (A). Filled gray and black line show isotype control and target expression, respectively. Alternatively, CD8α⁺ and CD8α⁻ DC were co-cultured with CFSE-labeled RAG2$^{-/-}$/OT-1 T cells for 3 d. The cross-priming activity of each DC subset was determined with sequential dilution of CFSE (B) and IFNγ production (C). IFNγ was measured by CBA assay. The data shown are representative of two independent experiments. Err bar shows SD.

CD8α⁺ DC where TLR3 is expressed in vivo. Peritoneal (PEC) Mf and bone marrow-derived DC[22] usually phagocytoze polyI:C and deliver them into the endosome. In mouse CD8α⁺ DC direct internalization of polyI:C has remain unproven. Using labeled polyI:C and anti-mouse TLR3 mAb, 11F8,[22] we checked whether the exogenously-added polyI:C encountered with TLR3 in CD8α⁺ DC in vitro. TLR3 (green) was merged with TexasRed-polyI:C 30–120 min after polyI:C stimulation in the culture (**Fig. 6A**). The quantities of CD8α⁺ and CD8α⁻ DC where FITC-polyI:C was incorporated were determined by FACS analysis (**Fig. 6B**). Thus, the process by which polyI:C injected reaches the endosomal TLR3 is delineated in the CD8α⁺ DC.

Discussion

PolyI:C is an analog of virus dsRNA, and acts as a ligand for TLR3 and RIG-I/MDA5. PolyI:C has been utilized as an adjuvant for enhancement of antitumor immunity for a long time.[29] However, the mechanistic background of the therapeutic potentials of polyI:C against cancer has been poorly illustrated. It induces antitumor NK activation through DC-NK cell-to-cell interaction when CD8α⁺ DC TLR3 is stimulated in the spleen.[11] Besides myeloid cells, however, some tumor cell lines express TLR3 and dsRNA targeting tumor cells may affect the growth rate of tumors,[30] where the receptor-interacting protein (RIP) pathway is involved downstream of TICAM-1.[31] Here we showed evidence that polyI:C injection facilitates maturation of TLR3-positive CD8α⁺ DC (i.e., APC) to trigger CTL induction against exogenous soluble Ags including EG7 lysate or OVA. The TICAM-1 adaptor for TLR3 and IRF-3/7 are involved in the cross-presentation signal in CD8α⁺ DC, but the molecule/mechanism downstream of TICAM-1 that governs cross-presentation remains elusive. Since most of the tumor-associated Ags (TAA) are predicted to be liberated from tumor cells

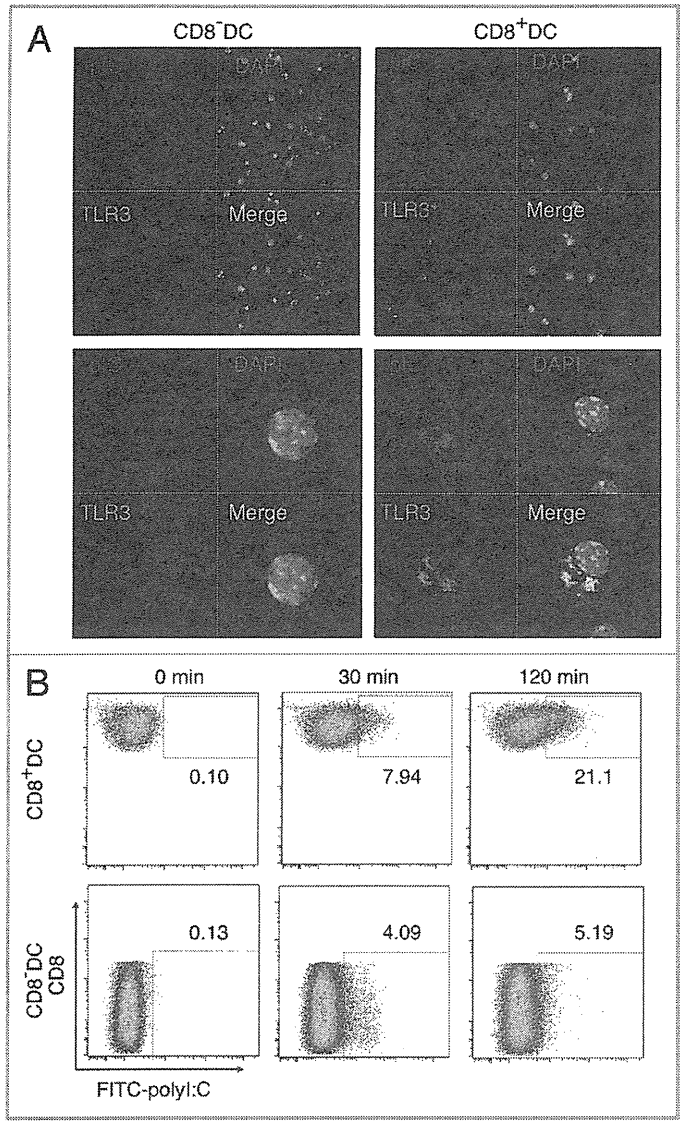

Figure 6. PolyI:C encounters TLR3 in CD8α⁺ DC. CD8α⁺ and CD8α⁻ DC were isolated by FACSAriaII and stimulated with 20 μg/ml TexasRed-polyI:C for 2 h. Then cells were stained with Alexa647-antiTLR3 and subjected to confocal microscopic analysis (A). Alternatively, splenic DC isolated by MACS were incubated with FITC-polyI:C for the time shown in figure and analyzed the degrees of polyI:C uptake by FACS (B). Data shown are the representative of three independent experiments.

as soluble Ags, the TICAM-1 pathway in CD8α⁺ DC would be crucial for driving of tumor-specific CTL around the tumor microenvironment. In any route of polyI:C injection, this is true as shown first in this study. Although TICAM-1 is an adaptor of other cytoplasmic sensors, DDX1, DDX21 and DHX36,[32] the antitumor CTL responses are merely relied on TLR3 of CD8α⁺DC in this system. Taken together with previous reports,[11,12] TICAM-1 signaling triggers not only NK activation but also CTL induction.

TLR3 and MDA5 are main sensors for dsRNA and differentially distributed in myeloid cells.[33,34] TLR3 is limitedly expressed in myeloid, epithelial and neuronal cells,[33] whereas MDA5 is ubiquitously expressed including non-myeloid stromal cells.[33] Several reports suggested that i.v. injection of polyI:C predominantly stimulate the stromal cells which express IFNAR,[26] thereby robust type I IFN are liberated from these cells to be a systemic response including cytokinemia and endotoxin-like shock.[35,36] Both TLR3 and MDA5 link to the IRF-3/7-activating kinases leading to the production of IFNα/β.[37,38] Once IFNα/β are released, IFNAR senses it to amplify the Type I IFN production,[39] and reportedly this amplification pathway involves cross-priming of CD8 T cells in viral infection.[18] Tumor progression or metastasis can be suppressed through the IFNAR pathway.[40] These scenarios may be right depending on the conditions employed. Our message is related to what signal pathway is fundamentally required for induction of antitumor CTL in DC. The CTL response is almost completely abrogated in TICAM-1$^{-/-}$ and IRF-3/7$^{-/-}$ mice, but largely remains in IPS-1$^{-/-}$ and IFNAR$^{-/-}$ mice when Ag and polyI:C are extrinsically administered. The results are reproducible in some other tumor-implant models (data not shown), and even in IFNAR$^{-/-}$ mice, TICAM-1-specific genes are upregulated to confer tumor cytotoxicity (**Fig. S6**, Azuma et al., unpublished data). In addition, the upregulation of these genes is independent of IPS-1 knockout in DC. Our results infer that the primary sensing of dsRNA in CD8α⁺ DC is competent to induce cross-presentation, which minimally involves the IPS-1 or IFNAR amplification pathway, at least at a low dose of polyI:C. Yet, subsequent induction of Type I IFN via the IFNAR may further amplify the cross-priming.[18,41] Further studies are needed as to which of the TICAM-1-inducible genes link to the cross-presentation in CD8α⁺ DC.

The main focus of this study was to identify the pathway for transversion of immature DC to the CTL-driving phenotype by co-administration of polyI:C with soluble Ag. The IPS-1 pathway, although barely participates in antitumor CTL driving, can upregulate CD40/CD86 co-stimulators on the membranes of splenic CD8α⁺ and CD8α⁻ DC in response to polyI:C, suggesting that MDA5 does function in the cytoplasm of splenic CD8α⁺ and CD8α⁻ DC to sense polyI:C. However, effective CTL induction happens only in CD8α⁺ DC when stimulated with polyI:C. CD8α⁺ DC express TLR3 but CD8α⁻ DC do not, and CD8α⁺ DC with no TLR3 fail to induce CTL, suggesting that integral co-stimulation by MDA5/IPS-1 is insufficient for DC to induce cross-priming of CD8 T cells: antitumor CTL are not induced until the TICAM-1 signal is provided in DC. At least, sole effect of the IPS-1 pathway and upregulation of co-stimulators on CD8α⁺ DC is limited for cross-priming and induction of antitumor CTL, which result partly reflects those in a previous report where IPS-1 and TICAM-1 harbor a similar potential for CD8 T cell proliferation when

polyI:C (Alum-containing) is employed as an adjuvant for CD8α+ DC to test proliferation of anti-OVA CTL.[21]

A question is why TICAM-1 is dominant to IPS-1 for response to exogenously-added polyI:C in CD8α+ DC. The answer is rooted in the difference of functional behavior between BMDC and CD8α+ DC. TLR3 levels are variable depending upon subsets of DC,[22] which affects DC subset-specific induction of cellular immune response. The high TLR3 expression (partly surface-expressed) is situated in CD8α+ DC before polyI:C stimulation, which is distinct from the properties of F4/80+ Mf and presumably BMDC of low TLR3 expression. The polyI:C-uptake machinery[15] appears to efficiently work in concert with the TLR3/TICAM-1 pathway in CD8α+ DC and this tendency is diminished when CD8α+ DC are pretreated with Alum + polyI:C.[21] Furthermore, there are functional discrepancies between CD8α+ splenic DC and GM-CSF-induced BMDC, which appears to reflect the difference of their TLR3 levels.[22] These results on CD8α+ DC encourage us to develop dsRNA adjuvant immunotherapy supporting TAA soluble vaccines for cancer applicable to humans, which possess the counterpart of CD8α+ DC.

There are two modes of dsRNA-mediated DC maturation, intrinsic and extrinsic modes that are governed by the IPS-1 and TICAM-1 pathways, respectively.[9,34] It is important to elucidate the in vivo qualitative difference in the two pathways in tumor-loading mice. TLR3+ DC/Mf are responsible for CTL driving via an extrinsic route in viral infection.[34] Previous data suggested that dsRNA in infectious cell debris, rather than viral dsRNA produced in the cytoplasm of Ag-presenting cells or autophagosome formation, contribute to fine tuning of DC maturation through extrinsic dsRNA recognition.[16] It is reported that dsRNA-containing debris are generated secondary to infection-mediated cell death,[41] and DC phagocytose by-stander dead cells. Likewise, soluble tumor Ags released from tumor cells usually are extrinsically taken up by APC in patients with cancer.[42] If CTL are successfully induced in therapeutic biotherapy targeted against cancer cells, this extrinsic TICAM-1 pathway must be involved in the therapeutic process.

Cross-presentation occurs in a TAP-dependent[43] and -independent fashions.[44,45] The peptides are transported by TAP into the endoplasmic reticulum (ER) and loaded onto MHC Class I for presentation at the cell surface. ER and phagosome might fuse each other for accelerating cross-presentation.[46] Another possibility is that cross-presentation occurs in early endosomes where TLR3 resides. This early endosome cross-presentation does not always depend on TAP[42-44] but requires TLR stimulation.[34] TLR4/MyD88 pathway is involved in the TAP-dependent early endosome model,[43] where recruitment of TAP to the early endosomes is an essential step for the cross-presentation of soluble Ag. These models together with our genechip analysis of polyI:C-stimulated BMDC suggested that some ER-associated proteins are upregulated in BMDC by polyI:C-TICAM-1 pathway. The results infer that the TLR3/TICAM-1 rather than the TLR4/MyD88 pathway more crucially participates in cross-presentation in response to dsRNA or viral stimuli and facilitates raising CTL antitumor immunity in APC.

Although multiple RNA sensors couple with TICAM-1 and signal to activate the Type I IFN-inducing pathway,[25] at least TLR3 in the CD8α+ DC are critical in CTL driving. CD8α+ DC are a high TLR3 expresser, while BMDC express TLR3 with only low levels.[22] CD8α- DC do not express it.[22] The Ag presentation and TLR3 levels in CD8α+ DC appear reciprocally correlated with the phagocytosing ability of DC. Although the TLR3 mRNA level is downregulated secondary to polyI:C response after maturation, this may not be related to the CD8α+ DC functions. Yet, polyI:C might interact with other cytoplasmic sensors for DC maturation.[32,47]

The route of administration and delivery methods may be important for culminate the polyI:C adjuvant function. The toxic problem has not overcome in the adjuvant therapy using polyI:C[35,36] and this is a critical matter for clinical introduction of dsRNA reagents to immunotherapy. The most problematic is the life-threatening shock induced by polyI:C. Recent advance of polyI:C study suggests that PEI-jet helps efficient uptake of polyI:C into peritoneal macrophages.[48] LC (poly-L-lysine and methylcellulose) has been used as a preservative to reduce the toxic effect of polyI:C.[49] Nanotechnological delivery of polyI:C results in efficient tumor regression.[50] There are many subsets of DC that can be defined by surface markers, and selecting an appropriate administration route can target a specific DC subset. The route for s.c. administration usually mature dermal/epidermal DC or Langerhans cells.[51,52] Some DC subsets with unique properties specialized to CTL induction would work in association with the route of polyI:C administration. Attempting to develop more harmless and efficient dsRNA derivatives will benefit for establishing human adjuvant immunotherapy for cancer.

Materials and Methods

Mice. TICAM-1$^{-/-}$ and IPS-1$^{-/-}$ mice were made in our laboratory and backcrossed more than eight times to adapt C57BL/6 background.[12] IRF-3/7$^{-/-}$ and IFNAR$^{-/-}$ mice were kindly provided by T. Taniguchi (University of Tokyo, Tokyo, Japan). TLR3$^{-/-}$ mice were kindly provided by S. Akira (Osaka University, Osaka, Japan). Rag2$^{-/-}$ and OT-1 mice were kindly provided from Drs N. Ishii (Tohoku University, Sendai, Japan). Rag2$^{-/-}$/OT-1 mice were bred in our laboratory. All mice were maintained under specific pathogen-free conditions in the animal facility of the Hokkaido University Graduate School of Medicine. Animal experiments were performed according to the guidelines set by the animal safety center, Hokkaido University, Japan.

Cells. EG7 and C1498 cells were purchased from ATCC and cultured in RPMI1640/10% FCS/55 μM 2-ME/1 mM sodium pyruvate and RPMI1640/10% FCS/25 ng/ml 2-ME, respectively. Mouse splenocytes, OT-1 T cell, CD8α+ DC and CD8α- DC were harvested from the spleen and cultured in RPMI1640/10% FCS/55 μM 2-ME/10 mM HEPES.[41] B16D8 cells were cultured in RPMI/10% FCS as described previously.[12]

Reagents and antibodies. Ovalbumin (OVA) and polyI:C (polyI:C) were purchased from SIGMA and Amersham Biosciences, respectively. $OVA_{257-264}$ peptide (SIINFEKL: SL8)

and OVA ($H2K^b$-SL8) Tetramer were from MBL. Following Abs were purchased: anti-CD3ε (145-2C11), anti-CD8β (53-6.7), anti-CD11c (N418), anti-CD16/32 (93), anti-CD69 (H1.2F3) and anti-IFNγ(XMG1.2) Abs from BioLegend, anti-B220 (RA3-6B2), anti-CD4 (L3T4), anti-CD40 (1C10), anti-CD86 (GL1), and anti-MHC I-SL8 (25-D1.16) Abs from eBiosciences, anti-TCR-Vβ5.1/5.2 Ab and ViaProbe from BD Biosciences. The Rat anti-mouse TLR3 mAb (11F8) was kindly provided by David M. Segal (National Institute of Health, Bethesda, MD). To rule out LPS contamination, we treated OVA or other reagents with 200 μg/ml of Polymixin B for 30 min at 37°C before use. Texas Red- or FITC-labeled poly(I:C) was prepared using the 5' EndTag™ Nucleic Acid Labeling System (Vector Laboratories) according to the manufacturers instructions.

Tumor challenge and poly I:C therapy. Mice were shaved at the back and s.c. injected with 200 μl of 2×10^6 syngenic EG7 cells in PBS. Tumor volumes were measured at regular intervals by using a caliper. Tumor volume was calculated by using the formula: Tumor volume (cm^3) = (long diameter) × (short diameter)^2 × 0.4. A volume of 50 μl of a mixture consisting of the lysate of 2×10^5 EG7 cells with or without 50 μg of poly I:C (polyI:C) was s.c. injected around the tumor. We added no other emulsified reagent for immunization since we want to role out the conditional effect of the Ag/polyI:C. The treatments were started when the average of tumor volumes reached at 0.4–0.8 cm^3 and performed twice per week. EG7 lysate were prepared by three times freeze/thaw cycles (-140°C/37°C) in PBS, with removal of cell debris by centrifugation at 6,000 g for 10 min.[53] To deplete CD8 T cells, mice were i.p. injected with hybridoma ascites of anti-CD8β mAb. The dose of antibody and the treatment regimens were determined in preliminary studies by using the same lots of antibody used for the experiments. Depletion of the desired cell populations by this treatment was confirmed by FACS for the entire duration of the study.

Evaluation of T cell activity in tumor-bearing mice. Draining inguinal LN cells were harvested from tumor-bearing mice after 24 h from the last polyI:C treatment. The activity of T cells was evaluated by CD69 expression and IL-2/IFNγ production. These cells were stained with FITC-CD8α, PE-CD69, PerCP/Cy5.5-7AAD and APC-CD3ε. To check cytokine production, LN cells were cultured for 3 d in vitro in the presence or absence of EG7 lysates and IL-2 and IFNγ productions were determined by Cytokine Beads Array (CBA) assay (BD). To assess the cytotoxic activity of CTL, standard ^{51}Cr release assay was performed. For CTL expansion, 2.5×10^6 LN cells were co-cultured with 1.25×10^5 mitomycin C-treated EG7 cells in the presence of 10 U/ml IL-2 for 5 d. Then, LN cells were incubated with ^{51}Cr-labeled EG7 or C1498 cells for 4 h and determined cytotoxic activity. The cell-specific cytotoxicity was calculated with subtracting the cytotoxity for C1498 from for EG7 cells.

Antigen-specific T cell expansion in vivo. Mice were i.p. immunized with 1 mg of OVA and 150 μg of poly I:C. After 7 d, spleens were homogenized and stained with FITC-CD8α and PE-OVA Tetramer for detecting OVA-specific CD8 T cell populations. For intracellular cytokine detection, splenocytes were cultured with or without 100 nM OVA peptide (SIINFEKL; SL8) for 8 h and 10 μg/ml of Brefeldin A (Sigma-Aldrich) was added to the culture in the last 4 h. Then cells were stained with PE-anti-CD8α and fixed/permeabilized with Cytofix/Cytoperm (BD Biosciences) according to manufacturer's instruction. Then, fixed/permeabilized cells were further stained with APC-anti-IFNγ. Stained cells were analyzed with FACSCalibur (BD Biosciences) and FlowJo software (Tree Star).

In vivo CTL assay. The in vivo CTL assay was performed as described.[54] In brief, WT, TICAM-$1^{-/-}$, MAVS$^{-/-}$ and IRF-$3/7^{-/-}$ mice were i.v. administered with PBS, 10 μg of OVA or OVA with 50 μg of polyI:C. After 5 d, 2×10^7 target cells (see below) were i.v. injected to other irrelevant mice and 8 h later, the OVA-specific cytotoxicity was measured by FACSCalibur. Target cells were 1:1 mixture of 2 μM SL8-pulsed, 5 μM CFSE-labeled splenocytes and SL8-unpulesed, 0.5 μM CFSE-labeled splenocytes. OVA-specific cytotoxicity was calculated with a formula: {1-(Primed [$CFSE^{high}$(%)/$CFSE^{low}$(%)]/Unprimed [$CFSE^{high}$(%)/$CFSE^{low}$(%)]} × 100.

DC preparation. DCs were prepared from spleens of mice, as described previously.[55] In brief, collagenase-digested spleen cells were treated with ACK buffer and then washed with PBS twice. Then splenocytes were positively isolated with anti-CD11c MicroBeads. $CD11c^+$ cells were acquired routinely about ≥ 80% purity. Further, to highly purify $CD8\alpha^+$ and $CD8\alpha^-$ DCs, spleen DC were stained with FITC-CD8α, PE-B220, PE/Cy7-CD11c and PerCP5.5-7AAD. $CD8\alpha^+$ or $CD8\alpha^-$ $CD11c^+B220^-$ DCs were purified on FACSAriaII (BD). The purity of the cells was ≥ 98%.

OT-1 proliferation assay. Ten micrograms of OVA with or without 50 μg of polyI:C were i.v. injected to WT, TICAM-$1^{-/-}$, IPS-$1^{-/-}$ and DKO mice. After 4 h, $CD8\alpha^+$ or $CD8\alpha^-$ DC were purified from the spleen. 2.5×10^4 $CD8\alpha^+$ or $CD8\alpha^-$ DC were co-cultured with 5×10^4 1 μM CFSE-labeled Rag$2^{-/-}$/OT-1 T cells for 3 d in 96-well round bottom plate. These cells were stained with PE-anti-TCR-Vβ5.1,5.2 and APC-anti-CD3ε and T cell proliferation was analyzed by CFSE dilution using FACSCalibur. Additionally, IFNγ in the culture supernatant was measured by CBA assay.

Statistical analysis. P-values were calculated with one-way analysis of variance (ANOVA) with Bonferroni's test. Error bars represent the SD or SEM between samples.

Disclosure of Potenial Conflicts of Interest

No potential conflicts of interest were disclosed.

Acknowledgment

We are grateful to Drs. T. Taniguchi (University Tokyo, Tokyo), N. Ishii (Tohoku University, Sendai) and D.M. Segel (NCI, Bethesda) for providing us with IRF-$3/7^{-/-}$ mice, OT-1 mice and anti-monse TLR3 mAb, respectively. Invaluable discussions about the peptide vaccine therapy with Dr. N. Satoh (Sapporo Medical

University, Sapporo) are gratefully acknowledged. We thank Drs H. Takaki, J. Kasamatsu, H.H. Aly, and H. Shime in our lab for their critical comments on this study.

This work was supported in part by Grants-in-Aid from the Ministry of Education, Science, and Culture (Specified Project for Advanced Research, MEXT) and the Ministry of Health, Labor, and Welfare of Japan, and by the Takeda and the Waxmann Foundations. Financial supports by a MEXT Grant-in-Project "The Carcinogenic Spiral" is gratefully acknowledged.

Supplemental Materials

Supplemental materials may be found here: http://www.landesbioscience.com/journals/oncoimmunology/article/19893/

References

1. Iwasaki A, Medzhitov R. Regulation of adaptive immunity by the innate immune system. Science 2010; 327:291-5; PMID:20075244; http://dx.doi.org/10.1126/science.1183021
2. Seya T, Shime H, Ebihara T, Oshiumi H, Matsumoto M. Pattern recognition receptors of innate immunity and their application to tumor immunotherapy. Cancer Sci 2010; 101:313-20; PMID:20059475; http://dx.doi.org/10.1111/j.1349-7006.2009.01442.x
3. Akira S. Toll-like receptor signaling. J Biol Chem 2003; 278:38105-8; PMID:12893815; http://dx.doi.org/10.1074/jbc.R300028200
4. Kawai T, Akira S. The roles of TLRs, RLRs and NLRs in pathogen recognition. Int Immunol 2009; 21:317-37; PMID:19246554; http://dx.doi.org/10.1093/intimm/dxp017
5. Longman RS, Braun D, Pellegrini S, Rice CM, Darnell RB, Albert ML. Dendritic-cell maturation alters intracellular signaling networks, enabling differential effects of IFN-alpha/beta on antigen cross-presentation. Blood 2007; 109:1113-22; PMID:17018853; http://dx.doi.org/10.1182/blood-2006-05-023465
6. Shinohara ML, Kim JH, Garcia VA, Cantor H. Engagement of the type I interferon receptor on dendritic cells inhibits T helper 17 cell development: role of intracellular osteopontin. Immunity 2008; 29:68-78; PMID:18619869; http://dx.doi.org/10.1016/j.immuni.2008.05.008
7. Diebold SS. Recognition of viral single-stranded RNA by Toll-like receptors. Adv Drug Deliv Rev 2008; 60:813-23; PMID:18241955; http://dx.doi.org/10.1016/j.addr.2007.11.004
8. Matsumoto M, Oshiumi H, Seya T. Antiviral responses induced by the TLR3 pathway. Rev Med Virol 2011. Epub ahead of print. PMID:21312311; http://dx.doi.org/10.1002/rmv.680
9. Yoneyama M, Fujita T. RIG-I family RNA helicases: cytoplasmic sensor for antiviral innate immunity. Cytokine Growth Factor Rev 2007; 18:545-51; PMID:17683970; http://dx.doi.org/10.1016/j.cytogfr.2007.06.023
10. Seya T, Matsumoto M. The extrinsic RNA-sensing pathway for adjuvant immunotherapy of cancer. Cancer Immunol Immunother 2009; 58:1175-84; PMID:19184005; http://dx.doi.org/10.1007/s00262-008-0652-9
11. Akazawa T, Ebihara T, Okuno M, Okuda Y, Shingai M, Tsujimura K, et al. Antitumor NK activation induced by the Toll-like receptor 3-TICAM-1 (TRIF) pathway in myeloid dendritic cells. Proc Natl Acad Sci U S A 2007; 104:252-7; PMID:17190817; http://dx.doi.org/10.1073/pnas.0605978104
12. Ebihara T, Azuma M, Oshiumi H, Kasamatsu J, Iwabuchi K, Matsumoto K, et al. Identification of a polyI:C-inducible membrane protein that participates in dendritic cell-mediated natural killer cell activation. J Exp Med 2010; 207:2675-87; PMID:21059856; http://dx.doi.org/10.1084/jem.20091573
13. Perrot I, Deauvieau F, Massacrier C, Hughes N, Garrone P, Durand I, et al. TLR3 and Rig-like receptor on myeloid dendritic cells and Rig-like receptor on human NK cells are both mandatory for production of IFN-gamma in response to double-stranded RNA. J Immunol 2010; 185:2080-8; PMID:20639488; http://dx.doi.org/10.4049/jimmunol.1000532
14. Bevan MJ. Cross-priming for a secondary cytotoxic response to minor H antigens with H-2 congenic cells which do not cross-react in the cytotoxic assay. J Exp Med 1976; 143:1283-8; PMID:1083422; http://dx.doi.org/10.1084/jem.143.5.1283
15. Datta SK, Redecke V, Prilliman KR, Takabayashi K, Corr M, Tallant T, et al. A subset of Toll-like receptor ligands induces cross-presentation by bone marrow-derived dendritic cells. J Immunol 2003; 170:4102-10; PMID:12682240
16. Schulz O, Diebold SS, Chen M, Näslund TI, Nolte MA, Alexopoulou L, et al. Toll-like receptor 3 promotes cross-priming to virus-infected cells. Nature 2005; 433:887-92; PMID:15711573; http://dx.doi.org/10.1038/nature03326
17. Kono H, Rock KL. How dying cells alert the immune system to danger. Nat Rev Immunol 2008; 8:279-89; PMID:18340345; http://dx.doi.org/10.1038/nri2215
18. Le Bon A, Etchart N, Rossmann C, Ashton M, Hou S, Gewert D, et al. Cross-priming of CD8+ T cells stimulated by virus-induced type I interferon. Nat Immunol 2003; 4:1009-15; PMID:14502286; http://dx.doi.org/10.1038/ni978
19. Bennett SR, Carbone FR, Karamalis F, Miller JF, Heath WR. Induction of a CD8+ cytotoxic T lymphocyte response by cross-priming requires cognate CD4+ T cell help. J Exp Med 1997; 186:65-70; PMID:9206998; http://dx.doi.org/10.1084/jem.186.1.65
20. Shimizu K, Kurosawa Y, Taniguchi M, Steinman RM, Fujii S. Cross-presentation of glycolipid from tumor cells loaded with alpha-galactosylceramide leads to potent and long-lived T cell mediated immunity via dendritic cells. J Exp Med 2007; 204:2641-53; PMID:17923500; http://dx.doi.org/10.1084/jem.20070458
21. Kumar H, Koyama S, Ishii KJ, Kawai T, Akira S. Cutting edge: cooperation of IPS-1- and TRIF-dependent pathways in poly IC-enhanced antibody production and cytotoxic T cell responses. J Immunol 2008; 180:683-7; PMID:18178804
22. Jelinek I, Leonard JN, Price GE, Brown KN, Meyer-Manlapat A, Goldsmith PK, et al. TLR3-specific double-stranded RNA oligonucleotide adjuvants induce dendritic cell cross-presentation, CTL responses, and antiviral protection. J Immunol 2011; 186:2422-9; PMID:21242525; http://dx.doi.org/10.4049/jimmunol.1002845
23. Wang Y, Cella M, Gilfillan S, Colonna M. Cutting edge: polyinosinic:polycytidylic acid boosts the generation of memory CD8 T cells through melanoma differentiation-associated protein 5 expressed in stromal cells. J Immunol 2010; 184:2751-5; PMID:20164430; http://dx.doi.org/10.4049/jimmunol.0903201
24. Carbone FR, Bevan MJ. Induction of ovalbumin-specific cytotoxic T cells by in vivo peptide immunization. J Exp Med 1989; 169:603-12; PMID:2784478; http://dx.doi.org/10.1084/jem.169.3.603
25. Asano J, Tada H, Onai N, Sato T, Horie Y, Fujimoto Y, et al. Nucleotide oligomerization binding domain-like receptor signaling enhances dendritic cell-mediated cross-priming in vivo. J Immunol 2010; 184:736-45; PMID:20008287; http://dx.doi.org/10.4049/jimmunol.0900726
26. McCartney S, Vermi W, Gilfillan S, Cella M, Murphy TL, Schreiber RD, et al. Distinct and complementary functions of MDA5 and TLR3 in poly(I:C)-mediated activation of mouse NK cells. J Exp Med 2009; 206:2967-76; PMID:19995959; http://dx.doi.org/10.1084/jem.20091181
27. Watanabe A, Tatematsu M, Saeki K, Shibata S, Shime H, Yoshimura A, et al. Raftlin is involved in the nucleocapture complex to induce poly(I:C)-mediated TLR3 activation. J Biol Chem 2011; 286:10702-11; PMID:21266579; http://dx.doi.org/10.1074/jbc.M110.185793
28. Itoh K, Watanabe A, Funami K, Seya T, Matsumoto M. The clathrin-mediated endocytic pathway participates in dsRNA-induced IFN-beta production. J Immunol 2008; 181:5522-9; PMID:18832709
29. Talmadge JE, Adams J, Phillips H, Collins M, Lenz B, Schneider M, et al. Immunomodulatory effects in mice of polyinosinic-polycytidylic acid complexed with poly-L-lysine and carboxymethylcellulose. Cancer Res 1985; 45:1058-65; PMID:3155990
30. Conforti R, Ma Y, Morel Y, Paturel C, Terme M, Viaud S, et al. Opposing effects of toll-like receptor (TLR3) signaling in tumors can be therapeutically uncoupled to optimize the anticancer efficacy of TLR3 ligands. Cancer Res 2010; 70:490-500; PMID:20068181; http://dx.doi.org/10.1158/0008-5472.CAN-09-1890
31. Kaiser WJ, Offermann MK. Apoptosis induced by the toll-like receptor adaptor TRIF is dependent on its receptor interacting protein homotypic interaction motif. J Immunol 2005; 174:4942-52; PMID:15814722
32. Zhang Z, Kim T, Bao M, Facchinetti V, Jung SY, Ghaffari AA, et al. DDX1, DDX21, and DHX36 helicases form a complex with the adaptor molecule TRIF to sense dsRNA in dendritic cells. Immunity 2011; 34:866-78; PMID:21703541; http://dx.doi.org/10.1016/j.immuni.2011.03.027
33. Gitlin L, Barchet W, Gilfillan S, Cella M, Beutler B, Flavell RA, et al. Essential role of mda-5 in type I IFN responses to polyriboinosinic:polyribocytidylic acid and encephalomyocarditis picornavirus. Proc Natl Acad Sci U S A 2006; 103:8459-64; PMID:16714379; http://dx.doi.org/10.1073/pnas.0603082103
34. Matsumoto M, Seya T. TLR3: interferon induction by double-stranded RNA including poly(I:C). Adv Drug Deliv Rev 2008; 60:805-12; PMID:18262679; http://dx.doi.org/10.1016/j.addr.2007.11.005

35. Absher M, Stinebring WR. Toxic properties of a synthetic double-stranded RNA. Endotoxin-like properties of poly I, poly C, an interferon stimulator. Nature 1969; 223:715-7; PMID:5805520; http://dx.doi.org/10.1038/223715a0
36. Berry LJ, Smythe DS, Colwell LS, Schoengold RJ, Actor P. Comparison of the effects of a synthetic polyribonucleotide with the effects of endotoxin on selected host responses. Infect Immun 1971; 3:444-8; PMID:16557994
37. Sasai M, Shingai M, Funami K, Yoneyama M, Fujita T, Matsumoto M, et al. NAK-associated protein 1 participates in both the TLR3 and the cytoplasmic pathways in type I IFN induction. J Immunol 2006; 177:8676-83; PMID:17142768
38. Ishikawa H, Barber GN. STING is an endoplasmic reticulum adaptor that facilitates innate immune signalling. Nature 2008; 455:674-8; PMID:18724357; http://dx.doi.org/10.1038/nature07317
39. Taniguchi T, Takaoka A. A weak signal for strong responses: interferon-alpha/beta revisited. Nat Rev Mol Cell Biol 2001; 2:378-86; PMID:11331912; http://dx.doi.org/10.1038/35073080
40. Ogasawara S, Yano H, Momosaki S, Akiba J, Nishida N, Kojiro S, et al. Growth inhibitory effects of IFN-beta on human liver cancer cells in vitro and in vivo. J Interferon Cytokine Res 2007; 27:507-16; PMID: 17572015; http://dx.doi.org/10.1089/jir.2007.0183
41. Ebihara T, Shingai M, Matsumoto M, Wakita T, Seya T. Hepatitis C virus-infected hepatocytes extrinsically modulate dendritic cell maturation to activate T cells and natural killer cells. Hepatology 2008; 48:48-58; PMID:18537195; http://dx.doi.org/10.1002/hep.22337
42. Chaput N, Conforti R, Viaud S, Spatz A, Zitvogel L. The Janus face of dendritic cells in cancer. Oncogene 2008; 27:5920-31; PMID:18836473; http://dx.doi.org/10.1038/onc.2008.270
43. Burgdorf S, Schölz C, Kautz A, Tampé R, Kurts C. Spatial and mechanistic separation of cross-presentation and endogenous antigen presentation. Nat Immunol 2008; 9:558-66; PMID:18376402; http://dx.doi.org/10.1038/ni.1601
44. Shen L, Sigal LJ, Boes M, Rock KL. Important role of cathepsin S in generating peptides for TAP-independent MHC class I crosspresentation in vivo. Immunity 2004; 21:155-65; PMID:15308097; http://dx.doi.org/10.1016/j.immuni.2004.07.004
45. Kurotaki T, Tamura Y, Ueda G, Oura J, Kutomi G, Hirohashi Y, et al. Efficient cross-presentation by heat shock protein 90-peptide complex-loaded dendritic cells via an endosomal pathway. J Immunol 2007; 179:1803-13; PMID:17641047
46. Gagnon E, Duclos S, Rondeau C, Chevet E, Cameron PH, Steele-Mortimer O, et al. Endoplasmic reticulum-mediated phagocytosis is a mechanism of entry into macrophages. Cell 2002; 110:119-31; PMID:12151002; http://dx.doi.org/10.1016/S0092-8674(02)00797-3
47. Samuel CE. Antiviral actions of interferons. Clin Microbiol Rev 2001; 14:778-809; PMID:11585785; http://dx.doi.org/10.1128/CMR.14.4.778-809.2001
48. Wu CY, Yang HY, Monie A, Ma B, Tsai HH, Wu TC, et al. Intraperitoneal administration of poly(I:C) with polyethylenimine leads to significant antitumor immunity against murine ovarian tumors. Cancer Immunol Immunother 2011; 60:1085-96; PMID:21526359; http://dx.doi.org/10.1007/s00262-011-1013-7
49. Longhi MP, Trumpfheller C, Idoyaga J, Caskey M, Matos I, Kluger C, et al. Dendritic cells require a systemic type I interferon response to mature and induce CD4+ Th1 immunity with poly IC as adjuvant. J Exp Med 2009; 206:1589-602; PMID:19564349; http://dx.doi.org/10.1084/jem.20090247
50. Kitano S, Kageyama S, Nagata Y, Miyahara Y, Hiasa A, Naota H, et al. HER2-specific T-cell immune responses in patients vaccinated with truncated HER2 protein complexed with nanogels of cholesteryl pullulan. Clin Cancer Res 2006; 12:7397-405; PMID:17189412; http://dx.doi.org/10.1158/1078-0432.CCR-06-1546
51. Kushwah R, Hu J. Complexity of dendritic cell subsets and their function in the host immune system. Immunology 2011; 133:409-19; PMID:21627652; http://dx.doi.org/10.1111/j.1365-2567.2011.03457.x
52. Asano K, Nabeyama A, Miyake Y, Qiu CH, Kurita A, Tomura M, et al. CD169-positive macrophages dominate antitumor immunity by crosspresenting dead cell-associated antigens. Immunity 2011; 34: 85-95; PMID:21194983; http://dx.doi.org/10.1016/j.immuni.2010.12.011
53. Galea-Lauri J, Wells JW, Darling D, Harrison P, Farzaneh F. Strategies for antigen choice and priming of dendritic cells influence the polarization and efficacy of antitumor T-cell responses in dendritic cell-based cancer vaccination. Cancer Immunol Immunother 2004; 53:963-77; PMID:15146294; http://dx.doi.org/10.1007/s00262-004-0542-8
54. Durand V, Wong SY, Tough DF, Le Bon A. Shaping of adaptive immune responses to soluble proteins by TLR agonists: a role for IFN-α/β. Immunol Cell Biol 2004; 82:596-602; PMID:15550117; http://dx.doi.org/10.1111/j.0818-9641.2004.01285.x
55. Yamazaki S, Okada K, Maruyama A, Matsumoto M, Yagita H, Seya T. TLR2-dependent induction of IL-10 and Foxp3+ CD25+ CD4+ regulatory T cells prevents effective anti-tumor immunity induced by Pam2 lipopeptides in vivo. PLoS One 2011; 6:e18833; PMID:21533081; http://dx.doi.org/10.1371/journal.pone.0018833

Arch Virol
DOI 10.1007/s00705-013-1618-6

ORIGINAL ARTICLE

Dynamics of cellular immune responses in the acute phase of dengue virus infection

Tomoyuki Yoshida · Tsutomu Omatsu · Akatsuki Saito · Yuko Katakai · Yuki Iwasaki · Terue Kurosawa · Masataka Hamano · Atsunori Higashino · Shinichiro Nakamura · Tomohiko Takasaki · Yasuhiro Yasutomi · Ichiro Kurane · Hirofumi Akari

Received: 13 June 2012 / Accepted: 12 December 2012

Abstract In this study, we examined the dynamics of cellular immune responses in the acute phase of dengue virus (DENV) infection in a marmoset model. Here, we found that DENV infection in marmosets greatly induced responses of CD4/CD8 central memory T and NKT cells. Interestingly, the strength of the immune response was greater in animals infected with a dengue fever strain than in those infected with a dengue hemorrhagic fever strain of DENV. In contrast, when animals were re-challenged with the same DENV strain used for primary infection, the neutralizing antibody induced appeared to play a critical role in sterilizing inhibition against viral replication, resulting in strong but delayed responses of CD4/CD8 central memory T and NKT cells. The results in this study may help to better understand the dynamics of cellular and humoral immune responses in the control of DENV infection.

T. Yoshida and T. Omatsu contributed equally to this study.

Electronic supplementary material The online version of this article (doi:10.1007/s00705-013-1618-6) contains supplementary material, which is available to authorized users.

T. Yoshida · Y. Iwasaki · T. Kurosawa · M. Hamano · Y. Yasutomi · H. Akari
Tsukuba Primate Research Center, National Institute of Biomedical Innovation, 1-1 Hachimandai, Tsukuba, Ibaraki 305-0843, Japan

T. Yoshida (✉) · A. Saito · A. Higashino · H. Akari (✉)
Center for Human Evolution Modeling Research, Primate Research Institute, Kyoto University, Inuyama, Aichi 484-8506, Japan
e-mail: yoshida.tomoyuki.4w@kyoto-u.ac.jp

H. Akari
e-mail: akari.hirofumi.5z@kyoto-u.ac.jp

Published online: 05 February 2013

Introduction

Dengue virus (DENV) causes the most prevalent arthropod-borne viral infections in the world [29]. Infection with one of the four serotypes of DENV can lead to dengue fever (DF) and sometimes to fatal dengue hemorrhagic fever (DHF) or dengue shock syndrome (DSS) [12]. The serious diseases are more likely to develop after secondary infection with a serotype of DENV that is different from that of the primary infection. Infection with DENV induces a high-titered neutralizing antibody response that can provide long-term immunity to the homologous DENV serotype, while the effect of the antibody on the heterologous serotypes is transient [22]. On the other hand, enhanced pathogenicity after secondary DENV infection appears to be explained by antibody-dependent enhancement (ADE). Mouse and monkey experiments have shown that subneutralizing levels of DENV-specific antibodies actually enhance infection [1, 6, 11]. Thus, the development of an effective tetravalent dengue vaccine is considered to be an important public-health priority. Recently, several DENV vaccine candidates have undergone clinical trials, and most of them target the induction of neutralizing antibodies [20].

T. Omatsu · T. Takasaki · I. Kurane
Department of Virology I, National Institute of Infectious Diseases, 1-23-1 Toyama, Shinjuku-ku, Tokyo 162-8640, Japan

Y. Katakai
Corporation for Production and Research of Laboratory Primates, 1-1 Hachimandai, Tsukuba, Ibaraki 305-0843, Japan

S. Nakamura
Research Center for Animal Life Science, Shiga University of Medical Science, Seta Tsukinowa-cho, Otsu, Shiga 520-2192, Japan